Late Cenozoic deformation and uplift of the NE Tibetan Plateau: Evidence from high-resolution magnetostratigraphy of the Guide Basin, Qinghai Province, China

Xiaomin Fang[†]
Institute of Tibetan Plateau Research, Chinese Academy of Science, P.O. Box 2871, Beilin North Str., Beijing 100085, China, and *National Laboratory of Western China's Environmental Systems, Ministry of Education of China and College of Resources and Environment, Lanzhou University, Gansu 730000, China*

Maodu Yan
Rob Van der Voo[‡]
David K. Rea
Department of Geological Sciences, University of Michigan, Ann Arbor, Michigan 48109-1063, USA

Chunhui Song
National Laboratory of Western China's Environmental Systems, Ministry of Education of China and College of Resources and Environment, Lanzhou University, Gansu 730000, China

Josep M. Parés
Department of Geological Sciences, University of Michigan, Ann Arbor, Michigan 48109-1063, USA

Junping Gao
Junsheng Nie
Shuang Dai
National Laboratory of Western China's Environmental Systems, Ministry of Education of China and College of Resources and Environment, Lanzhou University, Gansu 730000, China

ABSTRACT

The Cenozoic intramontane Gonghe–Guide Basin in Qinghai Province, China, is tectonically controlled by the sinistral strike-slip framework of the Kunlun and Altyn Tagh–South Qilian faults in the northeastern Tibetan Plateau. The basin is filled with thick Cenozoic clastic sedimentary formations, which provide important evidence of the deformation of this part of the plateau, although they have long lacked good age constraints. Detailed magnetostratigraphic and paleontologic investigations of five sections in the Guide Basin and their lithologic and sedimentary characteristics allow us to divide a formerly undifferentiated unit (the Guide Group) into six formations (where ages are now magnetostratigraphically well established, they are given in parentheses): the Amigang (1.8–2.6 Ma), Ganjia (2.6–3.6 Ma), and Herjia formations (3.6 to ca. 7.0–7.8 Ma), and the older Miocene Ashigong, Garang, and Guidemen formations. These rocks document a generally upward coarsening sequence, characterized by increasing accumulation rates. Increasing gravel content and sizes of its components, changes of bedding dips and source rock types, and marginal growth faults collectively reflect accelerated deformation and uplift of the NE Tibetan Plateau after 8 Ma, punctuated by a sharp increase in sedimentation rate at ca. 3.2 Ma that reflects the boulder conglomerates of the Ganjia formation. Interestingly, much of the vergence of the compressional deformation in the basin is to the south, accommodated by a sequence of six thrusts (F1–F6), which become active one by one progressively later toward the south, undoubtedly contributing to the uplift of this part of the plateau. F1 likely initiated the Guide Basin due to crustal flexure in the Oligocene, F2 was active in the early Miocene, F4 and F5 at ca. 3.6 Ma, and F6 was active in the early Pleistocene. The detailed late Miocene and younger magnetostratigraphy allows us to place much improved time constraints on the deformation and, hence, uplift of northeastern Tibet, which, when compared with ages for events on other parts of the plateau, provides important boundary conditions for the geodynamical evolution of Tibet.

Keywords: Tibet, Neogene, magnetostratigraphy, Qinghai Province, plateau uplift.

INTRODUCTION

The northeastern part of the Tibetan Plateau, north of the Kunlun Shan, is delineated by the bordering mountain ranges of the NE Altyn Tagh and the Qilian Shan–Liupan Shan and contains a number of large intramontane basins such as the Qaidam, Qinghai Lake, Gonghe–Guide and Longzhong basins (Fig. 1A). The topography of this part of the plateau is marked by elevations between ~2500 and 4000 m, which is much lower than the typical ~4000–

[†]E-mail: fangxm@itpcas.ac.cn.
[‡]Corresponding author e-mail: voo@umich.edu.

GSA Bulletin; September/October 2005; v. 117; no. 9/10; p. 1208–1225; doi: 10.1130/B25727.1; 11 figures; 3 tables.

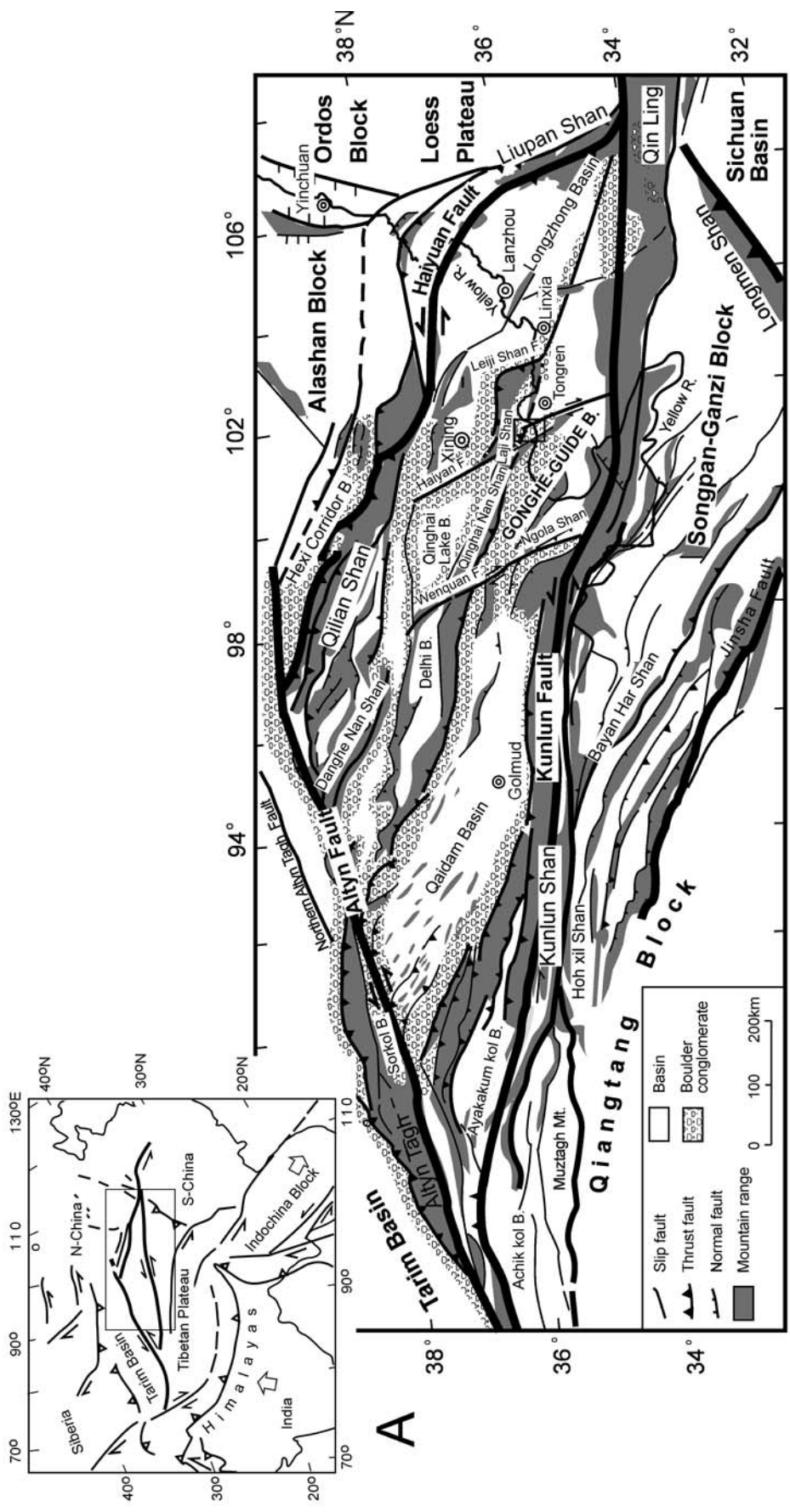

Figure 1. (A). Tectonic map of the NE Tibetan Plateau, compiled from Qinghai Geology Bureau (1989), Meyer et al. (1998), Song et al. (2001a) and Yin et al. (2002). The distribution of massive boulder conglomerates (molasse) is highlighted for emphasis. Our study area is centered around 101.5°E and 36°N. (*Continued on following page.*)

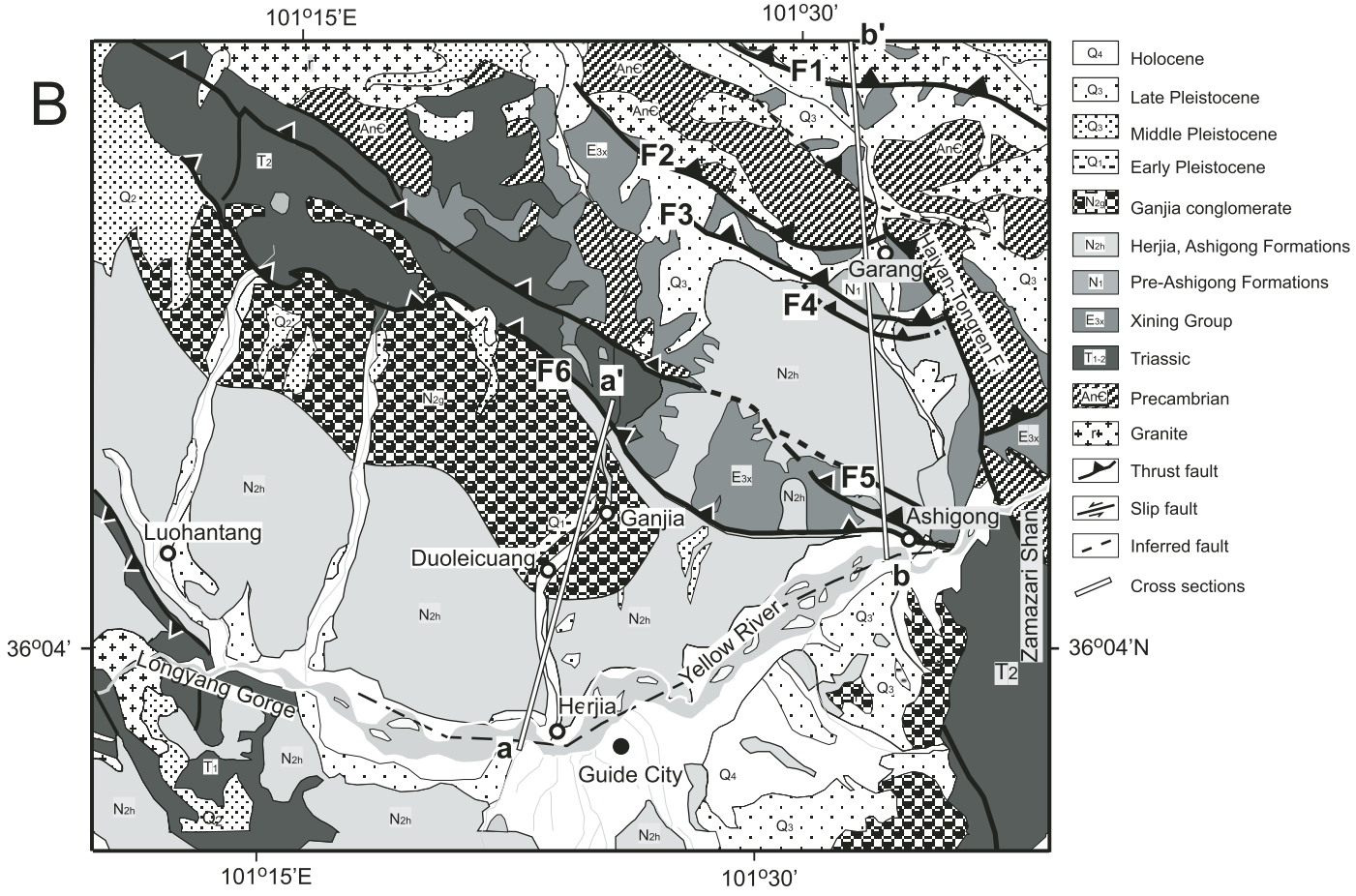

Figure 1 (*continued*). (B) Geologic map of part of the Guide Basin, showing the location of our main magnetostratigraphic profile (a–a′) as well as the location of a reconnaissance structural-geology profile (b–b′), where sampling for magnetostratigraphy was limited to a profile near the town of Ashigong. Thrust faults are labeled F1 through F6 from north to south. The original design of this map was adopted from that in Qinghai Geology Bureau (1989), but was modified by C.H. Song and X.M. Fang in minor ways by adding detail about the Neogene formations.

5000 m of the central and southern Tibetan Plateau. When and how this part of the Tibetan Plateau grew outward and upward has recently received increasing attention (Burchfiel et al., 1989, 1991; Molnar and Lyon-Caen, 1989; Tapponnier et al., 1990, 2001; Zhang et al., 1991; Gaudemer et al., 1995; Li et al., 1997a, 1997b; Li and Yang, 1998; Métivier et al., 1998; Meyer et al., 1998; Chen et al., 2000; Ritts and Biffi, 2000; Delville et al., 2001; George et al., 2001; Gilder et al., 2001; Jolivet et al., 2001; Sobel et al., 2001; Li et al., 2002; Yin et al., 2002; Fang et al., 2003; Wang et al., 2003) due to its relevance for Tibetan uplift models; even so, these models remain poorly understood because of a lack of widespread and precise constraints on the timing and rates of deformation and uplift.

Based largely on neotectonic, stratigraphic, and geomorphological information, Tapponnier and his colleagues (2001) concluded that the northeastern plateau is the most recently (Pliocene-Pleistocene) rising part of the Tibetan Plateau, which has grown obliquely starting with Eocene uplift of the southern plateau, followed by the central plateau in the Oligocene-Miocene. Within the northeastern plateau, deformation and uplift was driven by northeast-directed left-lateral slip along the Altyn Tagh fault, progressing from the southwest to the northeast and ending with today's growth in the Liupan Shan area (Fig. 1A). Much of the convergence has been absorbed by shortening along major WNW sinistral and NNW dextral transpressional faults (Burchfiel et al., 1989, 1991; Molnar and Lyon-Caen, 1989; Tapponnier et al., 1990, 2001; Gaudemer et al., 1995; Métivier et al., 1998; Meyer et al., 1998). Today, strike-slip deformation and northeastward movements dominate the northern part of the Tibetan Plateau, as demonstrated by earthquakes as well as global positioning system (GPS) measurements (Molnar and Lyon-Caen, 1989; Chen et al., 2000). Nevertheless, fission-track dating and preliminary Cenozoic magnetostratigraphy in the Qilian Shan and Altyn Tagh areas show that deformation and exhumation began in the Miocene or even in Eocene to Oligocene time (Gilder et al., 2001; George et al., 2001; Jolivet et al., 2001; Sobel et al., 2001; Yin et al., 2002; Wang et al., 2003). This does not preclude the contention of other researchers that slip along the Altyn Tagh fault and early deformation also occurred in the Mesozoic (Ritts and Biffi, 2000; Delville et al., 2001; Li et al., 2002). Because the Neogene sedimentary rocks in Tibet are excellent magnetostratigraphic recorders, it has been possible to document that early deformation in the Xining area and Linxia-Longzhong foreland basin (Fig. 1A) had reached this far east as early as late Oligocene (29 Ma; Fang et al., 2003; Dupont-Nivet et al., 2004; Horton et al., 2004), with increasing deformation intensity beginning in the Linxia Basin ca. 7.5 Ma (Fang et al., 2003).

The Gonghe–Guide Basin is a typical intramontane sedimentary basin akin to the larger

Source / Age	Loczy 1885*	Sun, 1934*	Lu, 1948*	Qinghai Regional Investigation Team, 1965*	Chinese Academy of Geology, 1979*	Regional Stratigraphic Table for the NW China, 1980*	Zhai & Cai, 1984 (Lanzhou Basin)	Fifth Qinghai Regional Geologic Team, 1989 *	Gu et al, 1992	Li et al., 1997b; Fang et al., 2003 Linxia Basin (Age in Ma)		This paper (Age in Ma)	
PLIOCENE	Guide Fm.	Xining Series	Guide Series	Guide Group	GUIDE GROUP: Linxia Fm.	GUIDE GROUP: Linxia Fm.	Linxia Fm.	Shangtan Fm.	Shangtan Fm.	1.77-2.58	Dongshan Fm.	GUIDE GROUP: 1.8-2.6	Amigang Fm.
			Tuosuhe Series							2.58-3.58	Jishi Fm.	2.6-3.6	Ganjia Fm.
										4.48-6	Hewangjia Fm.	3.6->7.0	Herjia Fm.
MIOCENE			Xianshuihe Series	Xining Group	Xianshuihe Fm.	Xianshuihe Fm.	Xianshuihe Fm.	L: Xiadongshan Fm.	Xiadongshan Fm.	6.0-7.56	Liushu Fm.		
								L: Charang Fm.	Charang Fm.	7.56-13.07	Dongxiang Fm.	>7.0->12	Ashigong Fm.
			Unnamed		Chetougou Fm.			M: Andang Fm.	Xianshuihe Fm.	13.07-14.68	Shangzhuang Fm.	<16?-19?	Garang Fm.
								M: Nengguo Fm.	Chetougou Fm.	14.68-21.4	Zhongzhuang Fm.	19?-20.8?	Guidemen Fm.
					Xiajia Fm.			E					
OLIGOCENE			Guyuan Series	Early Tertiary Series	XINING GROUP: Mahalagou Fm.	XINING GROUP: Qingshuiying Fm.	Upper Xining Group	Yehucheng Fm.		21.4-29	Tala Fm.	XINING GROUP	
							Lower Xining Group	Xiliugou Fm.					

Table 1. Stratigraphic nomenclature for the formations in the Guide and adjacent basins, as it evolved in the past 120 yr (earlier divisions are summarized in Zhai and Cai [1984] and Gu et al. [1992]), culminating in the divisions (with ages in Ma) for the Linxia Basin (Li et al., 1997b; Fang et al., 2003) and the Guide Basin (this study) at the right-hand side. *The references marked by the asterisk are not available to us, but the columns were copied from Zhai and Cai (1984) and Gu et al. (1992). E—Early; Fm—Formation; L—Late; M—Middle. Dashed/dotted lines indicate uncertain boundaries.

Qaidam Basin to the west (Fig. 1A). Incision by the Yellow River (Huang He) and its tributaries has exposed a rather complete Neogene sequence with numerous index fossils (Bohlin, 1937; Zhai and Cai, 1984; Zheng et al., 1985; Gu et al., 1992; Pan, 1994; Qiu and Qiu, 1995). However, despite the abundance of these fossils, the ages and regional correlation of the strata in this and adjacent basins have remained rather imprecise (Table 1). Our high-resolution magnetostratigraphic studies are designed to determine the ages of the molasse-type sedimentation in the northern Tibetan basins (Li et al., 1997b; Fang et al., 2003; Parés et al., 2003; Song et al., 2003), to attempt to arrive at a division into well-dated groups and formations, and to reconstruct the history of tectonic deformation and uplift of this part of the Tibetan Plateau.

GEOLOGICAL SETTING

The study area in the northeastern part of the Guide Basin is located to the north of the town of Guide on the Yellow River, just downstream from the famous Longyang Gorge (Fig. 1B). The surrounding Gonghe–Guide Basin is confined by the Ngola Shan to the west, Zamazari Shan to the east, the Qinghai Nan Shan–Laji Shan to the north, and the eastern Kunlun Shan to the south (Fig. 1). The east-west–trending, upthrusted, basement-cored ranges are controlled by left-lateral transpressional faults (Qinghai Geology Bureau, 1989), whereas to the west and east, the basin is bordered by two NNW-SSE right-lateral transpressional faults, the Wenquan and Haiyan-Tongren faults (Fig. 1A). Six prominent south-verging thrust faults (F1 to F6 in Fig. 1B) are found in this part of the basin on the south side of the Laji Shan, controlling the structures of the Neogene and older sedimentary strata. The Guide Basin occupies a surface area of ~1135 km^2, with elevations ranging from 2200 m (base level of the Yellow River in the city of Guide) to ~3600 m. The Yellow River and its tributaries cut ~900 m into the Cenozoic strata and the Triassic and Precambrian basement rocks and currently drain the entire Guide Basin, having formed seven Pleistocene terraces here and downstream (T2–T7; see also Li et al., 1997a).

The basement of the Guide Basin consists of Precambrian and Triassic rocks, mostly granites, phyllites, schists, and slates; these rocks are exposed in the bordering mountain ranges, which supplied the clastic components to the Cenozoic sedimentary sequence (Qinghai Geology Bureau, 1989; Fig. 1B). On the basis of field observations, we were able to divide the Cenozoic sequence into eight lithostratigraphic units; these are listed in Figure 2, with descriptions of lithology, fossils, and depositional environments, which will therefore not be repeated here. Throughout this manuscript, we will use unit numbers (1–8) as much as possible, and use the Chinese formation names sparingly, because the terminology of section names, formation names, and town or locality names may overlap and can become confusing.

The youngest of the lithostratigraphic units is a thin loess layer, varying in thickness from several meters to tens of meters. The underlying unit 2 is found mainly in the west and south

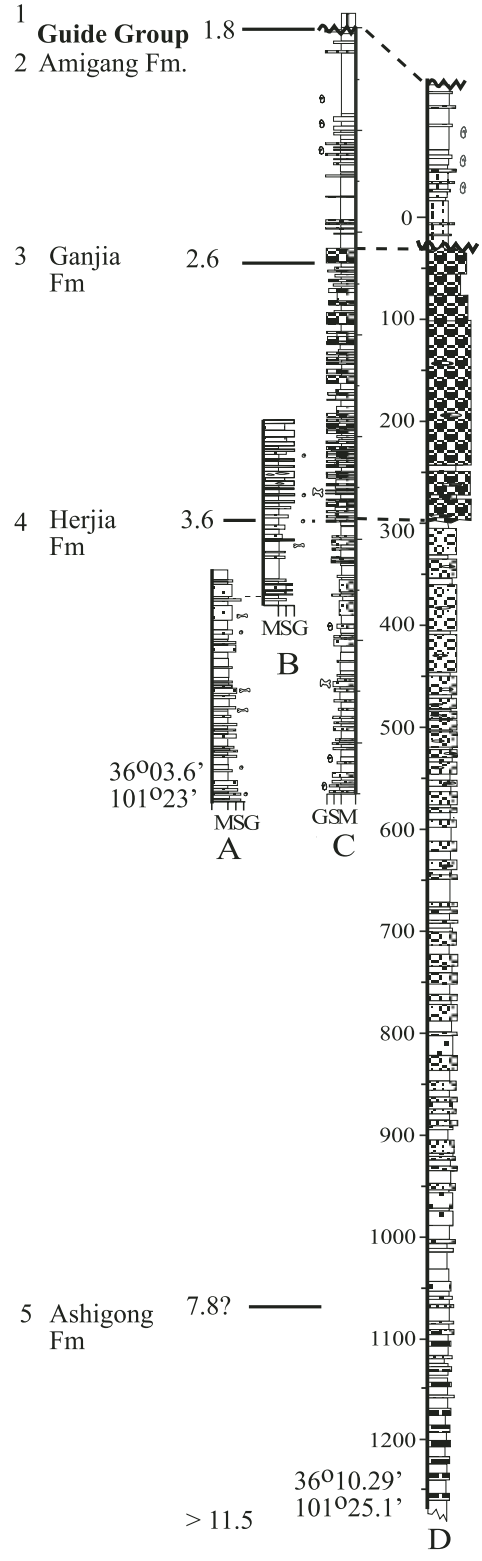

Unit	Age (Ma)	Depth (m)	Lithology	Fossils	Depositional environment
1 Guide Group 2 Amigang Fm.	1.8	0	Loess Light gray-bluish silt- & mudstones, intercalated with thin beds of yellowish sandstones, dark gray subangular poorly sorted pebble-conglomerates of slate or schist (~80%) and phyllite, granite and quartzite (~20%).	Mammals *Myospalax arvicolinus* and a horse (*Equus* sp.) (Song et al., 2001a).	Eolian Shallow lacustrine (Song et al., 2001a).
3 Ganjia Fm	2.6	100 200	Dark gray boulder fanglomerates near the basin's margin with lenses of finer-grained material (pebbly sandstones & siltstones). The north-dipping imbricated boulders, cobbles and pebbles are subrounded to subangular, mostly 5-30 cm in diameter, with a maximum of 100 cm; they comprise schist and phyllite (~45%), limestone (~13%), quartzite (~20%), granite (~5%), gneiss (~11%), and a few other lithologies (e.g., red sandstone).	*Hipparion* c.f. *Tchicoicum* (a three-toed horse) in the Amigang section (Gu et al., 1992; this study).	Alluvial fans, coarse-grained molasse, with boulders and pebbles derived from the nearby Laji Shan to the northeast (Song et al., 2001a).
4 Herjia Fm	3.6	300 400 500 600	Cross-bedded sandstones and pebbly conglomerates at the margins of the basin (brown to gray), but much finer-grained in the center of the basin. Near the town of Herjia, for instance, it consists of multicolored (dark red, brown, gray, grayish blue and light yellow) mudstones, siltstones and occasionally, sandstones.	(1) *Anancus sinensis*, *Axis shansius* and *Gazella kueitensis* in the upper layer; (2) *Mymomys* sp., *Ochotona* sp. and *Gazella kueitensis* in the middle layer (Fig. 5); (3) *Hipparion* sp. (three-toed horse), *Chilotherium* sp., *Gazella kueitensis* and *Axis shansius* in the lower layer (Zheng et al., 1985). In addition, *Hipparion* c.f. *Tchicoicum* (Lajigai section in Fig. 5) and *Anancus cuneatus* have been found in a few other places within the Guide Basin.	Braided-river – deltaic environments (Fothergill, 1998; Fothergill and Ma, 1999; Song et al., 2001a).
5 Ashigong Fm	7.8?	700 800 900 1000 1100 1200	Grayish-green and brown-dark reddish mudstones and siltstones irregularly interbedded with some sandstones and blue-gray mudstones.	In its upper part, *Hipparion* sp., *Gazella gaudryi* and a deer (*Cervavitus novorossiae*) (Fig. 4), with ages between 5.2 and 9 Ma (Song et al., 2001a); in the middle and upper parts of unit 5 at other localities, a number of mammals of late Miocene age were found, such as *Hipparion fossatum, H. Platyodus, Sinocastor, Goimphotherium, Chilitherium, Palaeotragus*, and *Gazella* (Gu et al., 1992).	Braided-river, lacustrine, and overbank floodplain (Song et al., 2001a).

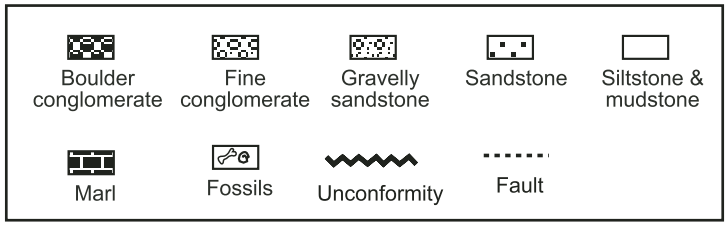

Figure 2. (*Continued on following page.*)

Unit	Age (Ma)	Depth (m)	Lithology	Fossils	Depositional environment
6 Garang Fm	< 16	0 E	The upper part has brownish-red muddy sandstone, intercalated with some grayish green sandstone.	*Kubanochoerus cf. lantiensis* (Gu et al., 1992).	Braided river systems (Song et al., 2001a).
	Upper	100			
	N36°08.38' E101°34.76' ~ 17?	0 F	The lower part consists of greenish gravelly sandstone interbedded with some conglomerate and dull yellowish- brownish sandy mudstone, as well as greenish-gray marl.		
	Lower	100			
	19?		Dark yellowish-gray fine conglomerates intercalated with some muddy sandstone. Pebbles are subangular to angular and poorly-sorted, with sizes of 3 -20 cm. They consist mostly of metamorphic sandstone, some quartzite, schist and limestone. Near the town of Ashigong, pebbles also consist of granite and Precambrian metamorphic rocks, which outcrop in the central Laji Shan. Unit 7 is strongly carbonate-cemented near Ashigong and manifests itself as an arced gate in topography due to the stream cutting through the center of the Ashigong fold (Fig. 3).	Pollen: *Chenopodiaceae*, *Artemisiaepollenites* and *Pinupollenites* (Gu et al., 1992).	Alluvial fans (Song et al., 2001a).
7 Guidemen Fm		200			
	20.8?	300 MSG			
8 **Xining Group**			Tan to orange-red sandy conglomerates, sandstones and silty mudstones.	N/A	N/A

Figure 2 (*continued*). Unit numbers, suggested formation names and ages (as derived from the results in this study), lithological columns, and descriptions of the lithologies, fossils, and depositional environments of the five studied sections. Four of these sections are located along the Nongchun River, indicated by profile a–a′ in Figure 1B. They are: (A) Herjia, (B) Lajigai, (C) Amigang, and (D) Ganjia. The older Ashigong section (F) is located at the southern end of profile b–b′ in Figure 1B. The Garang section (E) has not been studied magnetostratigraphically, but is included to show the lithologies of this unit.

of the basin where its thickness is the greatest, whereas it remains in only a few places to the south of thrust F6, such as north of Duoleicuang (shown as Q1 in Fig. 1B), where it has a thickness of ~217 m.

The conglomerates of unit 3 are found only to the south of thrust fault F5 and are featured prominently in Figure 1B. They have informally been called the Ganjia conglomerates previously (Song et al., 2001a; Parés et al., 2003). Unit 4 varies across the basin but it occurs only to the south of thrust fault F4. Numerous fossils have been found in unit 4; they are listed in Figure 2.

Unit 5 is very thick and well exposed in the northeastern part of the basin along the profile b–b′ between the towns of Ashigong and Garang to the south of thrust F4 and west of the Haiyan-Tongren transpressional fault (Fig. 1B). Unit 6 consists of an upper and a distinct lower part, is >300 m thick at Garang near the foot of the Laji Shan, and thins southward to ~100 m at Ashigong. Unit 7 is a distinct, cemented, fine-grained conglomerate 110–150 m thick.

The oldest Cenozoic formation in the basin is unit 8. Its magnetic properties are not included in this study, and so it is left in our Table 1 and figures as the Xining Group, as previously named by other workers. Unit 8 is widely distributed near the northeastern margins of the basin and on the top of the Laji Shan (E_{3x} in Fig. 1B).

SAMPLING AND MEASUREMENTS

We collected samples for magnetostratigraphy in two major and three minor sections; their lithological columns are shown alongside the unit descriptions in Figure 2. The major ones are referred to as the Ganjia and Amigang sections and these are located along the Nongchun River, north of the towns of Herjia and Guide (a–a′ in Fig. 1B). The shorter Lajigai and Herjia sections are located farther south along the Nongchun River, near the villages of Duoleicuang and Herjia (Fig. 1B); when we discuss the magnetostratigraphic results of these sections below, they will be summarized with their polarity records combined into one figure. Parts of the 220 m Herjia section have been studied previously by Song et al. (2003) and Parés et al. (2003). In order to relate the Herjia section to the much longer Ganjia and Amigang sections, a second short section was sampled at Lajigai between Herjia and Amigang. A marker bed, which can be traced in all these sections, has been used to control section correlation. To the east, at the south end of the b–b′ profile (Fig. 1B), the Ashigong section was sampled near the town of Ashigong (see also Fig. 3) in order to obtain preliminary indications of its magnetostratigraphy, fully realizing that this section, as can be seen in Figure 3, is far from ideal because of the presence of several faults. A future sampling program is planned for a more complete and thorough magnetostratigraphic study of units 5 and older.

The total sampled portion of the Ganjia section is 1288 m thick and contains strata from units 2–5. A steeply northward dipping thrust fault, F6, separates the Cenozoic from the upthrusted basement rocks of the Laji Shan to the north (Fig. 1B). The total sampled thickness of the Amigang section is 750 m; it contains units 2–4.

The sampled portion of the Lajigai section is 180 m thick and contains the lower part of unit 3 and the upper part of unit 4, whereas the Herjia section is 227 m thick and contains an upper-third part of unit 4. The Herjia locality is famous for its well-preserved fossil mammals (Fig. 2), excavated from caves dug into three layers within this section itself.

The provisional Ashigong section starts at the top at a fault below unit 5 and bottoms at the unconformity between units 7 and 8. It is located

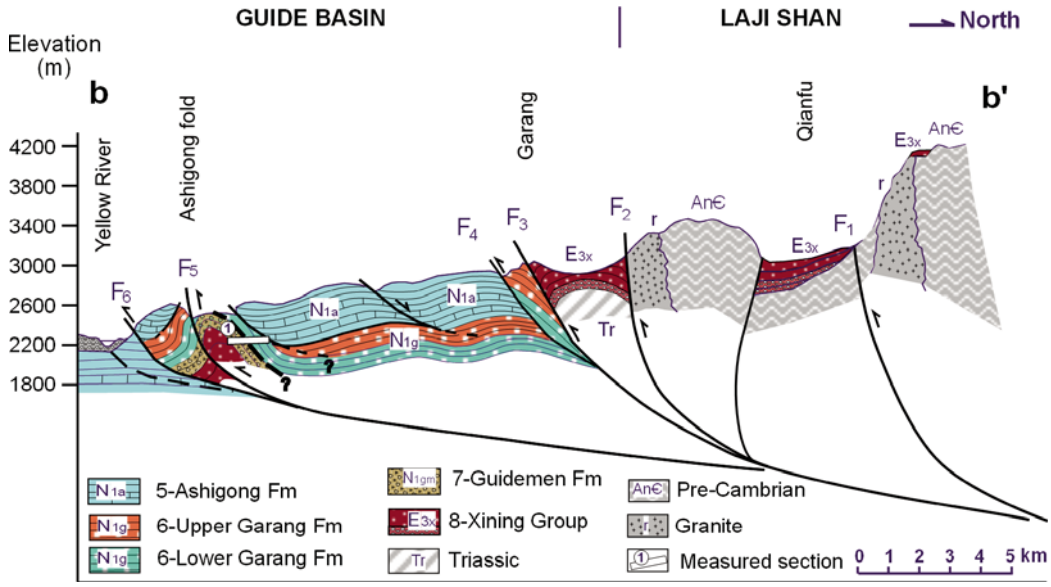

Figure 3. Cross section b–b′ (see Fig. 1B for location) along the valley through the towns of Ashigong and Garang. The section sampled for magnetostratigraphy is on the north limb of the Ashigong fold. Thrusts are labeled (F1–F6), whereas normal faults are not labeled, and faults of uncertain nature near our sampled section are denoted with a question mark. The section matches only approximately the geology portrayed in the (older-vintage) map of Figure 1B, and was constructed on the basis of field measurements by C.H. Song.

along the north limb of a fold near Ashigong at the southern end of profile b–b′ (Figs. 1B and 3). It is 280 m thick and contains unit 7 and the lower part of unit 6. Unit 7 is separated from unit 6 by a fault, which appears to have only minor displacement. It could not be decided in the field whether the fault is a thrust or a normal fault, and a similar ambiguity marks the fault at the top of this section. Both faults are therefore marked with a question mark in Figure 3. These faults render this section less desirable for magnetostratigraphic work, as already noted.

Samples were mostly collected at intervals of 2 m, but due to the presence of conglomerates (e.g., in units 3 and 7) sample spacing had to be up to 4–5 m in some parts of the sections, depending on the occurrence of lenses of siltstone to fine-grained sandstone that could be collected for magnetostratigraphy. At each sampling level (site), at least three oriented cubic samples (2 × 2 × 2 cm) were obtained. This resulted in an initial collection of more than 2500 samples, followed by a subsequent collection of samples, wherever it appeared necessary to resolve magnetostratigraphic ambiguities. In the end, the total number of samples was 423 × 3, 250 × 3, 81 × 3, 113 × 3, and 88 × 3 samples, from the Ganjia, Amigang, Lajigai, Herjia, and Ashigong sections, respectively. Remanence intensities and directions of the first, second, and third sets of the samples were measured with a JR-5a spinner magnetometer at Lanzhou University, with a 2G cryogenic magnetometer at the Beijing Institute of Geology and Geophysics of the Chinese Academy of Science, and a 2G cryogenic magnetometer at the University of Michigan, respectively. Only thermal demagnetization was used and proceeded in 18 steps between ~25 °C and 700 °C on pilot samples, and in ~10–16 steps up to 680 °C or until the intensity was near the noise level of the cryogenic magnetometer for the remaining samples. For sites that yielded ambiguous polarity results or that recorded what looked like reversals or polarity transitions defined by a single sample (~20% of total sites), an additional two specimens were collected at the appropriate sites with deeper digging in the field. These supplemental samples were measured only with the 2G cryogenic magnetometers.

PALEOMAGNETIC AND MAGNETOSTRATIGRAPHIC RESULTS

The intensity of the natural remanent magnetization (NRM) of the clastic sedimentary samples is 10^{-2}–10^{-3} A/m; NRM intensities of limestones are low and their directions are unstable and could not be used. Representative thermal demagnetization diagrams of samples from four sections are shown in Figure 4. Demagnetization diagrams for the fifth section, at Herjia, have been published before (Parés et al., 2003). Most samples show uncomplicated demagnetization behavior: after removal of a low unblocking temperature component by 150–350 °C, a characteristic magnetization (ChRM) is isolated and decays nearly linearly to the origin. Maximum unblocking temperatures of 680 °C indicate that hematite is the carrier of the magnetization in all sections, but the presence of magnetite is suggested as well by an accelerated decay of the magnetization between 500–550 and 580 °C (Fig. 4). A slight difference in direction can be seen between the magnetizations presumably carried by magnetite and hematite (e.g., samples GJ630, GJ1281, AMG671, AMG42, and AMG460, in Fig. 4), but we have not observed such directions to have opposite polarities. ChRM component directions have been calculated for all samples using principal component analysis, guided by visual inspection of the orthogonal demagnetization diagrams such as shown in Figure 4. Remanence directions of the samples generally agreed between the three laboratories unless the samples were unstable and showed noisy demagnetization behavior (~15% of the total). For unstable and noisy samples, the two sets measured with the 2G cryogenic magnetometers were nearly the same, but differed for samples measured with the JR-5a spinner magnetometer; these sites (sampling levels) were discarded. The final mean direction for each site was obtained by Fisher averaging of the ChRM directions from the three samples for that site.

Specimens not included in our magnetostratigraphic analysis were rejected on the basis of three criteria: (1) ChRM directions could not be determined because of ambiguous or noisy orthogonal demagnetization diagrams. (2) ChRM directions revealed maximum angular deviation (MAD) angles greater than 15°. (3) Specimens revealed magnetizations with virtual geomagnetic pole (VGP) latitude values less than 30°. A total of 83 sites (20%), 46 sites (18%), 16 sites (20%), 26 sites (23%), and 21 sites (24%) in the Ganjia, Amigang, Lajigai, Herjia, and Ashigong sections, respectively, were so excluded (Table 2).

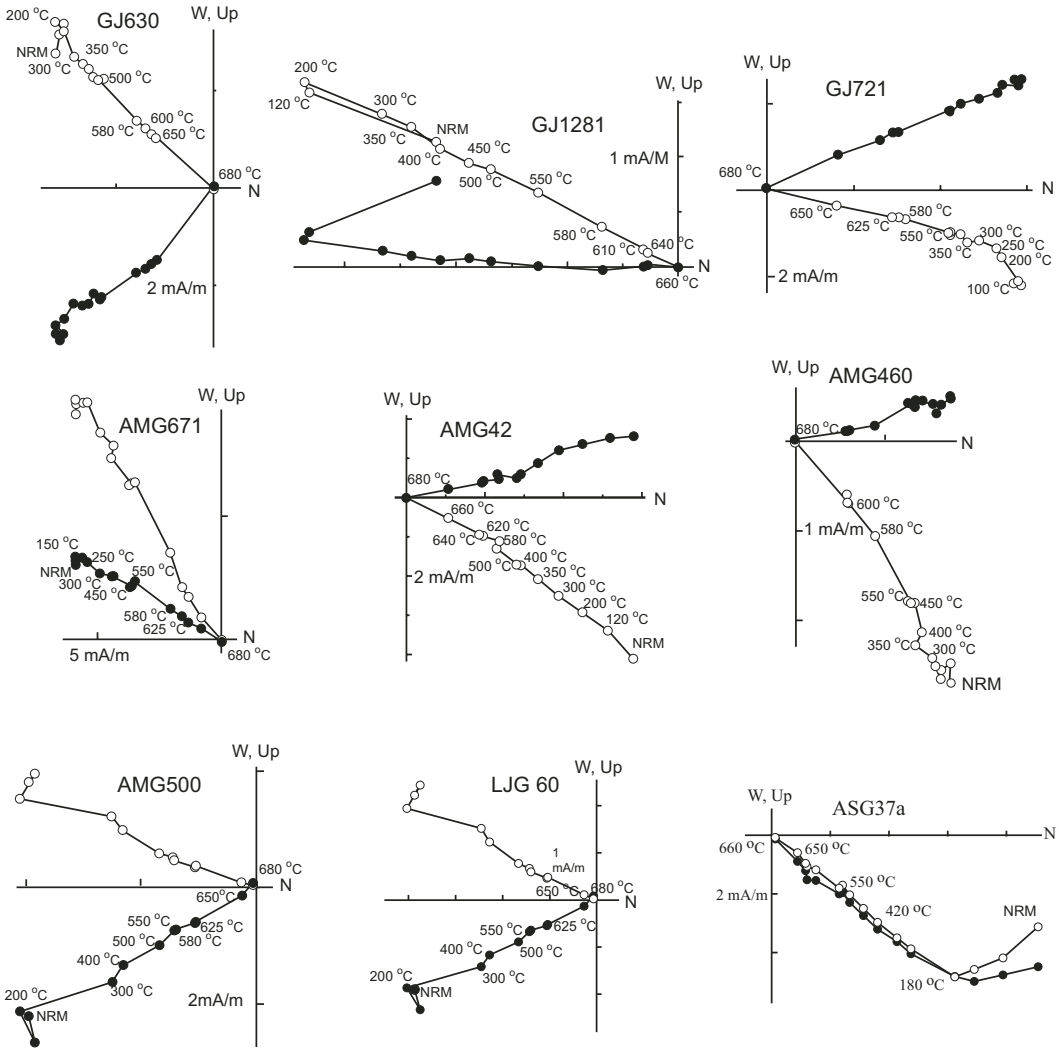

Figure 4. Representative thermal orthogonal demagnetization diagrams for samples from the Ganjia (GJ), Amigang (AMG), Lajigai (LJG), and Ashigong (ASG) sections. Open (closed) symbols represent vertical (horizontal) projections; intensities are given in mA/m. NRM—natural remanent magnetization.

Figure 5 shows the dual-polarity ChRM directions and the reversal tests of four sections (Ganjia, Amigang, Lajigai, and Ashigong). We used a statistical bootstrap technique (Tauxe, 1998) to examine possible non-Fisherian distributions of ChRM vectors, and to characterize the associated uncertainties for both normal and reversed ChRM directions, as illustrated in Figure 5. The histograms of Cartesian coordinates of bootstrapped means (Tauxe, 1998) allow us to determine a 95% level of confidence (ovals around the means in Fig. 5) and demonstrate that the bootstrap reversal test is positive for all four sections.

Virtual geomagnetic pole latitudes (VGP-lat) were determined by calculating site-mean directions and their corresponding pole positions; the present-day latitudes of these pole locations are plotted in Figures 6 and 7 as VGP-lat. Single sites indicating a different polarity from those of sites above and below (e.g., the site at 1185 m in the Ganjia section in Fig. 6) have been included in the VGP latitude columns but were not used in the "observed polarity" columns.

There are a total of 17 normal and 17 reversed polarity intervals recorded in the Ganjia section and 12 normal and 11 reversed polarity intervals in the Amigang section, marked as N1–17, R1–17, N'1–12 and R'1–11, respectively (Fig. 6). The observed polarities can be correlated with confidence to the geomagnetic polarity time scale (GPTS) of Cande and Kent (1995) for most of the two sections. N'1 is correlated to the Olduvai Normal (Chron 2n), N'2 to the Reunion subchron, N1–3 and N'3–6 to the Gauss interval (Chron 2An), R4–R8 and R'6–R'10 to the Gilbert interval with predominantly reversed polarities (Chrons 2Ar–3r), and N8–9 and N'11–12 to Chron 3An. A slight uncertainty in this correlation is that R9 at ~730 m is very thin, even though it is based on three stratigraphic levels. But more disconcertingly, the proffered correlation runs into ambiguities below R11, and an alternative correlation to that presented in Figure 6 is possible, in which N14 would correspond to Chron 4n. But the long normal polarity interval of N16 appears best correlated to the similarly long Chron 5n, and not with Chron 4An. Interestingly, there are even some single sample levels within N16 (see VGP latitudes at ~1155 and 1185 m), which resemble cryptochrons reported multiple times for Chron 5n (e.g., Garcés et al., 1996; Li et al., 1997b; Roberts and Lewis-Harris, 2000; Fang et al., 2003). For the time being, we recognize the uncertainty of our correlation between unit 5 and the GPTS, but stress that whichever of the two alternatives is chosen, the age of the bottom of the Ganjia section is likely to be ca. 10–11 Ma.

The magnetostratigraphy of the much shorter Lajigai and Herjia sections (Fig. 7) is relatively straightforward and correlates, as expected from the laterally equivalent results in the Ganjia and Amigang sections, with the

TABLE 2. PALEOMAGNETIC DATA FROM THE FIVE MAGNETOSTRATIGRAPHIC SECTIONS, GUIDE BASIN

Formation (unit)	Section	*N*/*n*	w/o TC		TC		α_{95}	*k*	Lat	Long
			Dec (°)	Inc (°)	Dec (°)	Inc (°)			(°N)	(°E)
Normal polarities										
Amigang (2)	AMG	72/24	358.2	31.4	355.4	31.7	10.9	8.5	70.7	294.4
	GJ	8/0								
Ganjia (3)	AMG	65/30	1.5	42.5	1.2	46.0	10.5	7.0	81.3	273.9
	GJ	56/27	9.5	40.7	2.4	44.0	8.0	13.0	79.6	269.0
	LJG	39/23	6.7	30.3	353.8	42.0	12.2	7.0	77.1	307.1
Herjia (4)	AMG	113/32	6.2	42.2	9.4	43.9	8.7	10.0	76.9	240.4
	GJ	237/69	5.0	31.4	355.9	44.0	5.2	12.5	79.2	301.1
	LJG	42/5	354.3	35.0	351.2	32.7	40.1	10.5	70.2	306.5
	HJ	113/33	7.8	42.0	8.4	43.8	8.3	10.0	77.4	244.0
Ashigong (5)	GJ	122/77	8.5	36.4	2.8	51.9	4.5	13.5	85.8	246.5
Garang (6)	ASG	43/26	66.2	28.3	29.6	37.5	10.7	8.0	60.1	213.9
Guidemen (7)	ASG	45/26	52.5	32.6	45.9	17.9	12.1	7.0	61.0	200.0
Reversed polarities										
Amigang (2)	AMG	72/37	179.0	–42.4	178.8	–44.8	9.0	8.0	–80.4	107.4
	GJ	8/6	183.4	–44.7	174.4	–46.1	29.4	6.0	–80.2	131.7
Ganjia (3)	AMG	65/21	177.6	–38.8	176.7	–42.0	15.2	5.0	–77.9	115.5
	GJ	56/11	163.8	–45.3	155.5	–46.5	12.8	13.5	–67.7	176.3
	LJG	39/6	193.7	–26.2	184.7	–34.3	30.4	6.0	–72.3	86.2
Herjia (4)	AMG	113/60	184.3	–41.7	185.8	–44.8	5.5	11.5	–79.2	72.1
	GJ	237/124	190.0	–31.6	184.4	–44.5	3.8	11.5	–79.5	78.9
	LJG	42/31	183.8	–32.2	188.8	–36.0	9.3	9.0	–72.2	72.9
	HJ	113/54	183.3	–41.7	185.9	–44.0	5.5	13.0	–78.6	73.1
Ashigong (5)	GJ	122/26	192.1	–33.0	188.7	–45.8	9.4	10.0	–78.5	58.5
Garang (6)	ASG	43/5	252.3	–33.5	217.1	–22.8	28.8	5.0	48.1	218.7
Guidemen (7)	ASG	45/10	230.1	–37.6	217.9	–34.4	21.5	6.0	52.6	208.7
Combined										
Amigang (2)	AMG	72/61			357.1	39.8	6.6	8.0	76.4	292.4
	GJ	8/6			354.4	46.1	29.4	6.0	80.2	311.7
	Mean	80/67			357.1	40.4	6.1	8.0	76.8	292.8
Ganjia (3)	AMG	65/51			359.3	44.9	8.3	7.0	80.5	284.8
	GJ	56/38			354.9	45.4	7	12.0	79.9	307.9
	LJG	39/29			356.2	40.6	11.0	7.0	76.8	296.5
	Mean	160/118			357.3	44.5	4.7	8.0	79.9	295.0
Herjia (4)	AMG	113/92			7.0	44.5	4.6	11.0	78.5	247.8
	GJ	237/193			1.4	44.4	3.1	12.0	80.0	273.7
	LJG	42/36			7.1	35.8	8.8	9.0	72.7	258.0
	HJ	113/87			6.8	43.9	4.6	12.0	78.2	249.7
	Mean	505/406			3.7	44.1	2	12.0	79.4	262.7
Ashigong (5)	GJ	122/103			4.4	50.5	4.1	12.0	84.0	242.2
Garang (6)	ASG	43/31			31.1	35.2	9.8	8.0	58.0	214.7
Guidemen (7)	ASG	45/36			43.9	22.5	10.4	6.0	43.6	212.0

Note: Summary of the paleomagnetic data, by formation (and stratigraphic unit number in parentheses, see text), by section, and by polarity for each of the five sections, where *N* is the total number of sites collected from a formation and *n* is the number of sites used in the calculation of a (normal, reversed, or combined polarity) mean direction. Abbreviations: AMG—Amigang section, ASG—Ashigong section, GJ—Ganjia section, HJ—Herjia section, LJG—Lajigai section; TC—corrected for the tilt of the strata; w/o TC—without tilt correction; Dec, declination; Inc, inclination; *k* and α_{95} are the statistical parameters associated with the means; Lat and Long—latitude and east-longitude of the paleomagnetic pole positions.

Gauss and Gilbert intervals, to the bottom in Chron 3An at ca. 6.3 Ma (Fig. 7). No polarity intervals appear to be missing.

In Figure 8 the four Nongchun Valley (a–a′) sections can be compared with each other and with a geological profile that ranges from the south-verging F6 thrust at the northern end, to the Yellow River at the profile's southern end. Note that the profile has a vertical exaggeration. In this profile, the magnetostratigraphic sections are represented by open bars, labeled with capital letters (A–B, C–D etc.) that correspond to those of the columns above it. Ages of the strata shown in this profile are derived from the magnetostratigraphy, which is relatively clear and unambiguous for ages younger than 6.2 Ma and has an uncertainty of about one million years in the bottom part of the Ganjia section (indicated by question marks in the correlation of G–H with the GPTS).

The magnetostratigraphy of the Ashigong section is shown in Figure 9, and remains speculative because of a lack of anchoring of the observed polarity intervals to well-established correlations for younger strata, and, as already mentioned, because of the presence of a fault between units 5 and 6 on top of the section and another one between units 6 and 7 in the middle of the section. We include these very provisional results here to document that (1) normal polarity dominates, as would be the case for the GPTS segment between 17 and 21.3 Ma (Chrons 5Dn–6An.1n; see Fig. 9), and (2) to establish for the record that units 6 and 7 appear to be good polarity recorders, so that it will be worthwhile to seek better sections elsewhere in the Guide Basin in the future. We must also note that in Figure 9 the VGP latitudes are based on directions for which the declinations (~30–40°; see Table 2) are rotated counterclockwise to coincide with due north.

We used the jackknife technique (Tauxe and Gallet, 1991) to quantify the reliability of the magnetostratigraphy. The obtained jackknife parameters (J) have values of –0.0308 and –0.0684 in the Ganjia and the Amigang sections, respectively, which fall within the range of 0 to –0.5 recommended by Tauxe and Gallet (1991) for a robust magnetostratigraphic data set. The J values predict that both sections have recovered more than 95% of the true number of polarity intervals (Fig. 10).

CORRELATIONS OF MAGNETOSTRATIGRAPHY WITH FOSSILS

For the Amigang section, additional age constraints are provided by the fauna *Gazella kueitensis* and *Anancus sinensis* found in the upper part of unit 4 (Gu et al., 1992) (Fig. 6). These mammals have also been found in Chinese sediments elsewhere where they have been assigned to the Baodean stage (Zheng et al., 1985; Qiu and Qiu, 1995) (= ~Turolian at 5.2–9 Ma [Berggren and Van Couvering, 1974]), which approximately agrees with our magnetostratigraphic age determinations of 5–5.5 Ma for this part of the section. At a lower level, the Baodean mammals *Gazella gaudryi*, *Cervavitus novorossiae* and *Hipparion* sp. were found in the upper part of unit 5 in the Ganjia section (Fig. 6), and this provides further age constraints.

Figure 7 illustrates how the magnetostratigraphic age determinations of units 3 and 4 in the Herjia and Lajigai sections match the many Pliocene and late Miocene fossil mammals in these sections (Zheng et al., 1985; Song et al., 2003).

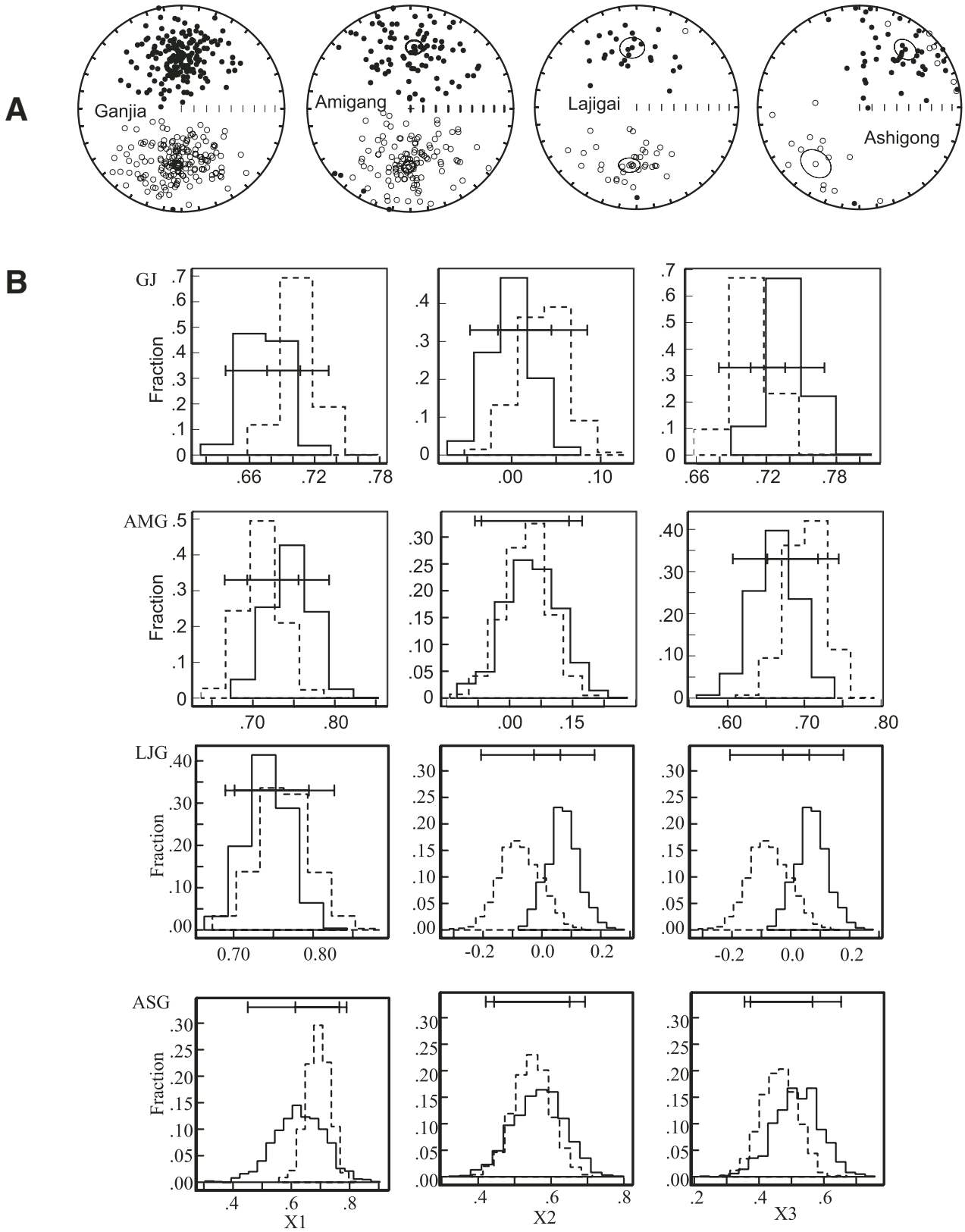

Figure 5. (A) Equal-area projections of the characteristic remanent magnetization (ChRM) directions and mean directions (with oval of 95% confidence) for the Ganjia, Amigang, Lajigai, and Ashigong sections determined with the bootstrap method (Tauxe, 1998). Downward (upward) directions are shown as filled (open) circles. (B) Bootstrap reversal test diagrams for the Ganjia (GJ), Amigang (AMG), Lajigai (LJG), and Ashigong (ASG) sections. Reversed polarity directions have been inverted to their antipodes to test for a common mean for the normal and reversed magnetization directions. The confidence intervals for all components overlap, indicating positive reversal tests.

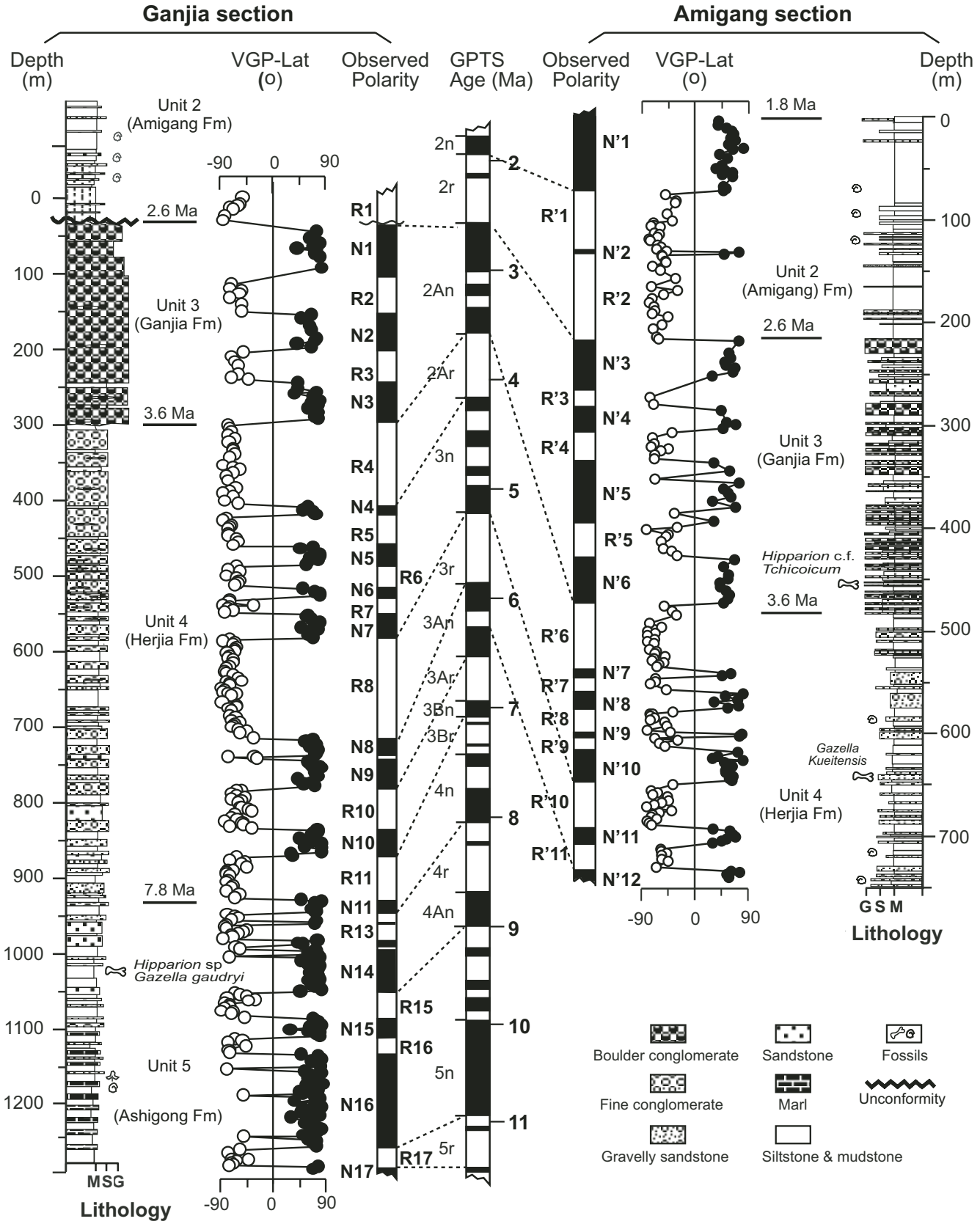

Figure 6. Magnetostratigraphic results versus lithostratigraphic position in the Ganjia and Amigang sections; for location see profile a–a′ in Figure 1B. MSG and GSM: M, mudstone and siltstone; S, sandstone; G, gravel and conglomerate. GPTS is the reference geomagnetic polarity time scale from Cande and Kent (1995). VGP-Lat (latitude) is explained in the text.

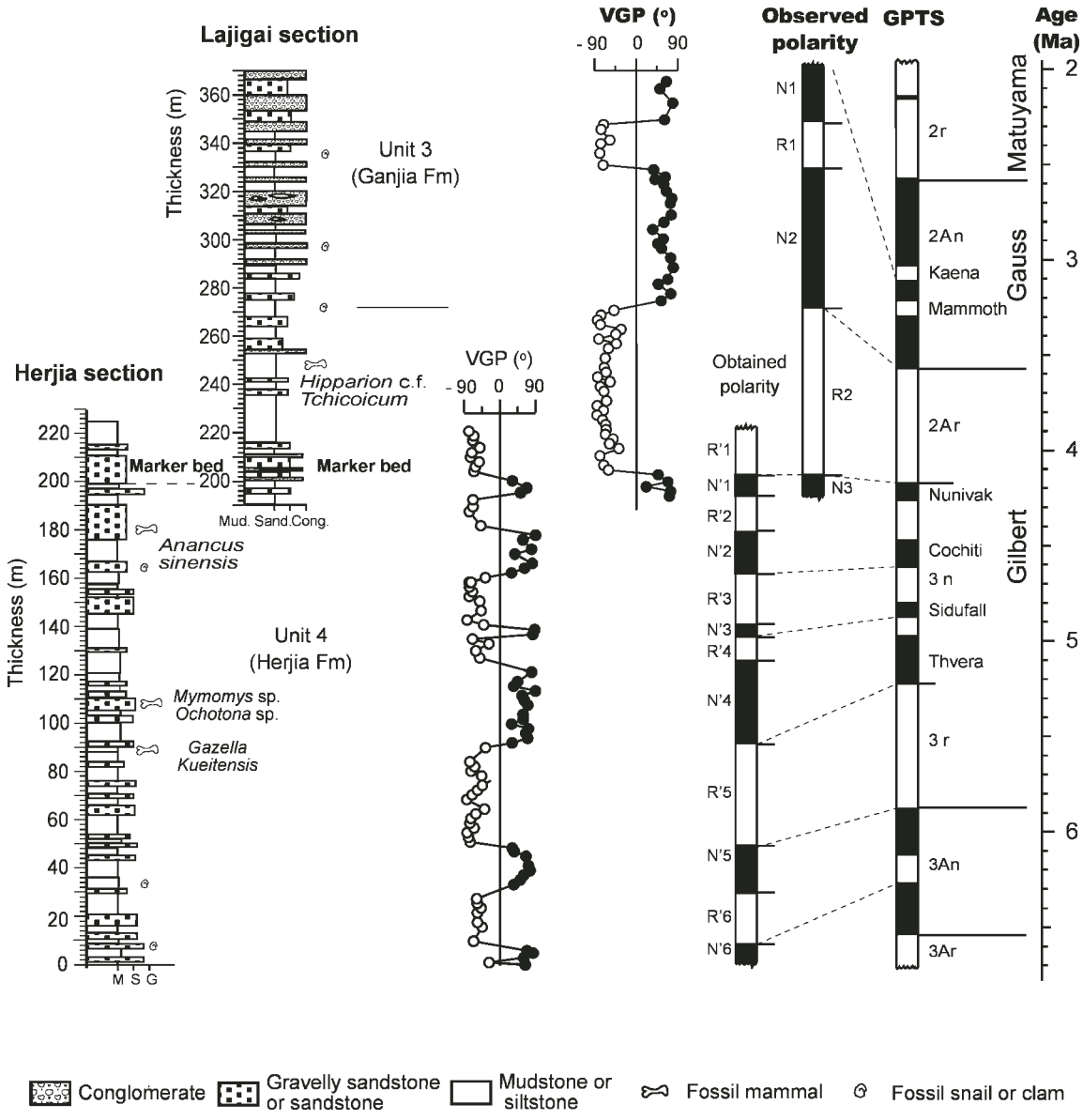

Figure 7. Magnetostratigraphic results versus lithostratigraphic position for the Herjia and Lajigai sections along the southern part of the Nongchun Valley in the Guide Basin; for location, see Figures 1B and 8. Other details are as in Figure 6.

The magnetostratigraphy of the Ashigong section (Fig. 9) is, as already noted, rather preliminary. Our field observations, as illustrated in Figure 3, indicate that the sampled strata of this section are older than unit 5 (N1a = Ashigong formation). Units 6 and 7 are therefore considerably older than the 10–11 Ma age of the lowest sampled part of unit 5 (the lowest unit in the Ganjia section in Fig. 6). As already mentioned, this suggested to us that units 6 and 7 recorded Chrons 5Dn through 6An.1r. We find support for our age assignment in the lithological resemblance of units 6 and 7 to apparently equivalent early-middle Miocene strata in the Longzhong Basin near Linxia, where bio- and magnetostratigraphical dating yields ages of 14.7–21.4 Ma (Fang et al., 2003) for the Zhongzhuang Formation (see Table 1). An early-middle Miocene pig (*Kubanochoerus cf. lantiensis*) found in unit 6 elsewhere in the Guide Basin and pollen in unit 7 (Fig. 2) support the early to middle Miocene age assignments (Gu et al., 1992).

If our magnetostratigraphic correlation is valid, it appears that the fault in the Ashigong section (at ~130 m in Fig. 9) does not represent a major stratigraphic gap, as not much section appears to be missing; however, it bears keeping in mind that this needs future confirmation by detailed sampling of parallel sections that have yet to be identified.

AGE DATES AND A REFINED DIVISION INTO FORMATIONS FOR THE NEOGENE STRATA

Considering the different names and imprecisely or poorly defined ages of Guide Group divisions presented in earlier work (Table 1), as recently as 1992, it is clear that any earlier division of the Guide Group into formations must be subject to revision. Based on our field

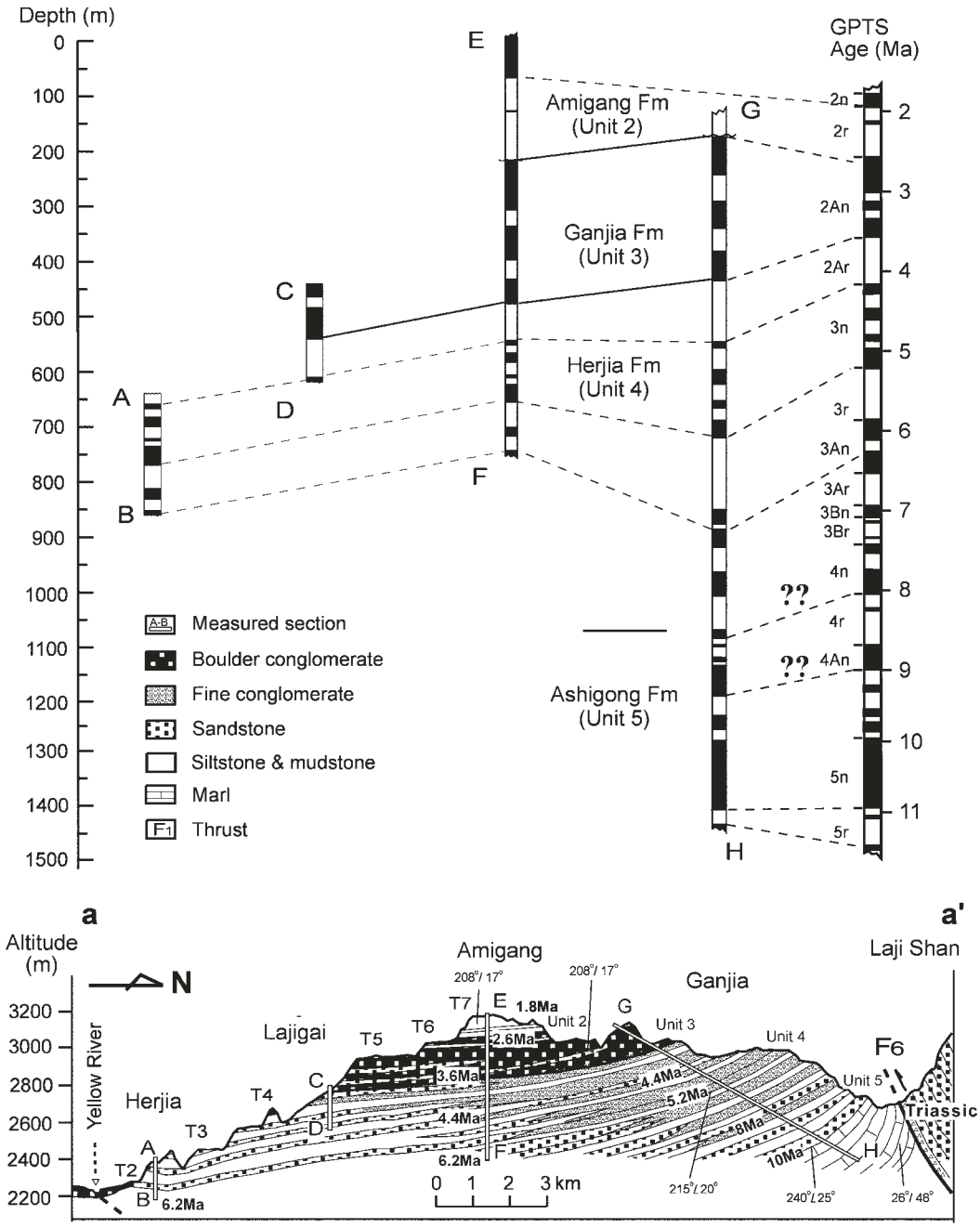

Figure 8. (Bottom) Cross section a–a′ (see Fig. 1B) along the Nongchun River, showing four of our sampled sections, where A–B represents the Herjia section, C–D the Lajigai section, E–F the Amigang section, and G–H the Ganjia section. The strata are inclined with diminishing dips to the southwest. Note the vertical exaggeration of the profile; selected dip directions and dips are shown. (Top) Correlation of the magnetostratigraphy (detailed in Figs. 6–7) of the four sampled sections, plotted versus relative depth (m) and compared with the geomagnetic polarity time scale (GPTS) of Cande and Kent (1995). Black is normal and white is reversed polarity. The Yellow River has incised more than 900 m after deposition of the early Pleistocene sedimentary strata (i.e., unit 2, now at the summit of Amigang mountain, at ~3180 m); note the seven Yellow River terraces T2–T7 of Pleistocene age (Li et al., 1997a). Ages shown in Ma have been derived from our magnetostratigraphic analyses and from Song et al. (2003) and Parés et al. (2003) at Herjia (section A–B). The correlation of unit 5 with the GPTS is not unambiguous and, hence, is marked by question marks for ages older than 6.2 Ma.

observations of the lithologies, and comparisons with strata in nearby basins (e.g., the Longzhong Basin near Linxia [Fang et al., 2003]), we have divided the sedimentary rocks in the Guide Basin into the 8 units already mentioned. Unit 1 is a thin loess layer of no more than some tens of meters in thickness; it is distributed mainly as a thin veneer on top of the Cenozoic and older formations and on Pleistocene river terraces. We did not include unit 1 in our magnetostratigraphic study, but its age is certainly within the Pleistocene.

Based on our magnetostratigraphy, geochronological ages of units 2 and 3 were determined with good confidence as 1.77–2.6 Ma for unit 2 and 2.6–3.6 Ma for unit 3. Ages for unit 4 range from 3.6 to either 7.8 (preferred) or to 7.0 Ma, depending on how one correlates the N9–N11 sequence of the observed magnetic polarities to the GPTS between Chrons 3An and 4n. For units 6–7, the ages are clearly early to middle Miocene, but more precise numerical age assignments at this time must remain tentative. Our best estimates are 7.8 to older than 12 Ma for unit 5, younger than 16–19 Ma for unit 6, and 19–20.8 Ma for unit 7. Collectively, these six units (2–7) form what we retain as the previously named Guide Group, with ages spanning nearly all of the Miocene and Pliocene, as well as the earliest Pleistocene.

Unit 3 is the massive and thick (~260 m) conglomeratic layer that forms the major upper cliffs along the Nongchun River north of Guide, where the strata dip gently (~17°) southwestward (see Fig. 8). Comparing the magnetostratigraphic columns of Figure 8, it can be seen that the thicknesses of units 3 and 4 diminish toward the south. Moreover, the massive conglomerates of unit 3 show decreasing average grain sizes also toward the southwest (compare the lithological columns

of Figs. 6 and 7). This late Pliocene conglomeratic unit has been interpreted as a coarse-grained molasse, with boulders and pebbles derived from the nearby Laji Shan to the northeast (Song et al., 2001a). Based on the age constraints now obtained for unit 3 (Ganjia formation), it can be correlated to other molasse-type conglomerates in adjacent basins, such as the Jishi Formation in the more easterly Longzhong Basin (see Fig. 1A for location; Li et al., 1997b; Fang et al., 2003), and the Pliocene molasses in the more westerly Qaidam Basin (Zhai and Cai, 1984; Métivier et al., 1998) or in the Hexi Corridor Basin north of the Qilian Shan (Song et al., 2001b). These other conglomerate occurrences have all been dated by magnetostratigraphy as time-equivalent to unit 3 (see Fang et al., 2004). Unit 3 has historically been part of the formations variously named Guide, Linxia, or Shangtan (see Table 1, with references as provided by Gu et al., 1992). More recently it has been called (informally) the Ganjia conglomerate (Song et al., 2001a; Parés et al., 2003). Because the Jishi molasse is named after the Jishi Shan, from where its cobbles and pebbles were derived, whereas the Ganjia conglomerates in the Guide Basin were derived mainly from the nearby Laji Shan, it appears to be preferable not to use the name of Jishi. Consequently, we name unit 3 the Ganjia Formation because of its location in our Ganjia section and the previously adopted informal use of this name.

Unit 4 is ~630 m thick in the apparently unabridged Ganjia section and its upper part is represented by the lower 262 m of the Amigang section and by 270 m of the Lajigai–Herjia sections (Figs. 4 and 5). It is early Pliocene and Messinian (late Miocene) in age; the precise numerical age of its base is uncertain (between 7.0 and 7.8 Ma). The sedimentary rocks have been interpreted as representing deposition in perennial braided-river–deltaic environments (Fothergill, 1998; Fothergill and Ma, 1999; Song et al., 2001a). Because unit 4 is thick and well exposed in the Herjia region, and because it contains numerous fossils there (Zheng et al., 1985), we name it the Herjia Formation.

Only the upper part (360 m) of unit 5 is represented in the Ganjia section, with an age mostly older than Messinian (older than 7.0 Ma). In the Ashigong section it has not (yet) been sampled. Unit 5 is characterized by distinct alternating multicolored (chiefly grayish-greenish and brown) beds of marls and mudstone-siltstone, and in the field we referred to these lacustrine strata as the "Zebra Beds." Similarly alternating multicolored layers are found in the Dongxiang Formation in the Longzhong Basin (Li et al., 1997b; Fang et al., 2003; see Table 1), but given the uncertainty as to whether the two basins

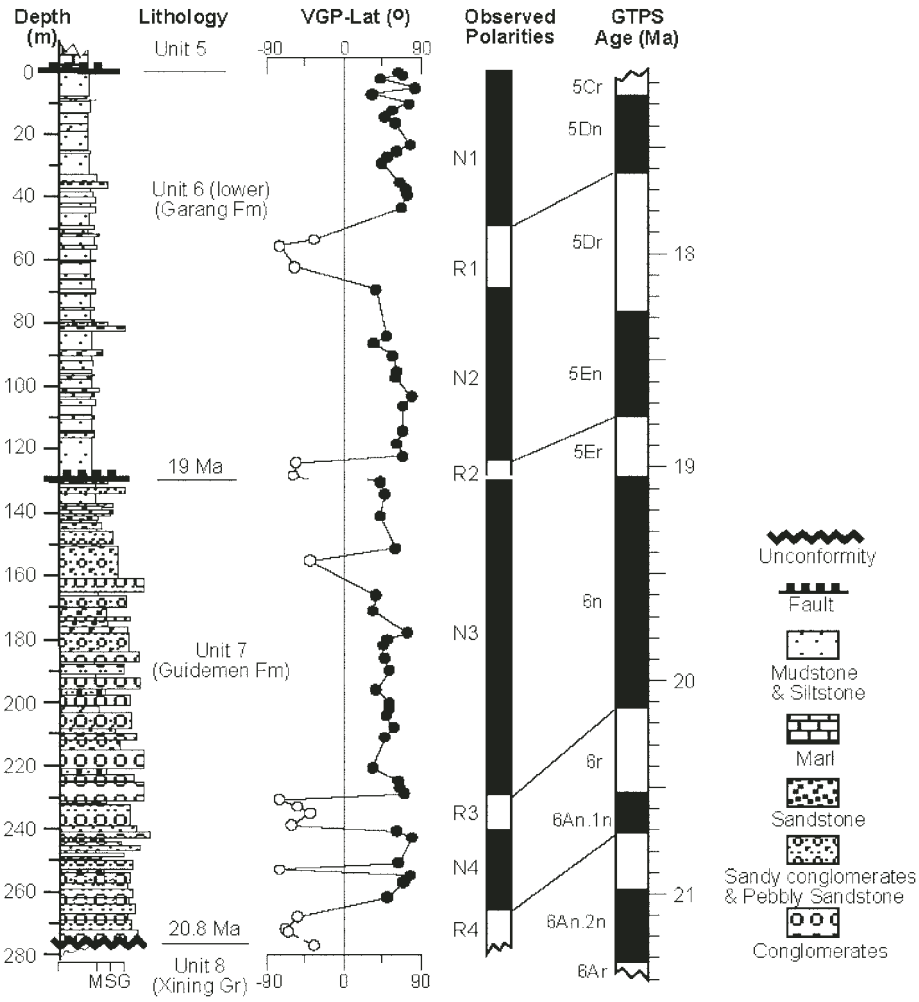

Figure 9. Magnetostratigraphic results versus lithostratigraphic position for the section near the town of Ashigong (for location see southern end of profile b–b′ in Fig. 1B). Other details are as in Figure 6. Faults of uncertain displacement style (normal or thrust?) were observed at the top and the middle of the section (see also Fig. 3), whereas the bottom of the section spans the unmistakable angular unconformity between the Guide and Xining Groups.

were part of the same depositional system, we prefer to give a new name to unit 5 and call it the Ashigong Formation. The Dongxiang Formation is reasonably well dated as 7.56–13 Ma, and contains the Sigou fauna thought to be 9–12.5 Ma (Fang et al., 2003). If unit 5 can be unambiguously correlated to the GPTS in a future study, correlation between these two units with their similar Serravallian-Tortonian (middle-late Miocene) fauna can be tested further.

The precise numerical ages of units 6 and 7 remain very speculative at this time, but the ages are reasonably constrained to be early-middle Miocene. Unit 6 is well exposed at Garang, with thicknesses of up to 200 m and ages tentatively estimated as falling between 16 and 19 Ma. These sediments record a braided-river environment, representing a transition from the earlier alluvial fan environment of unit 7 to the later lake system of unit 5 (Song et al., 2001a). We propose the name of Garang Formation for this unit.

Unit 7 is 147 m thick in the Ashigong section, with early Miocene ages (tentatively estimated as between 19 and 21 Ma), and represents an important early episode of conglomerate deposition. The unit has been thrusted southward in the Guide Gate area near Ashigong and in the valley manifests itself in the core of an anticlinal structure (called the Ashigong fold in Fig. 3). Because there is a pronounced angular unconformity below it and given that it consists mostly of alluvial fan deposits (Song et al., 2001a), unit 7 actually may provide a record of significant early

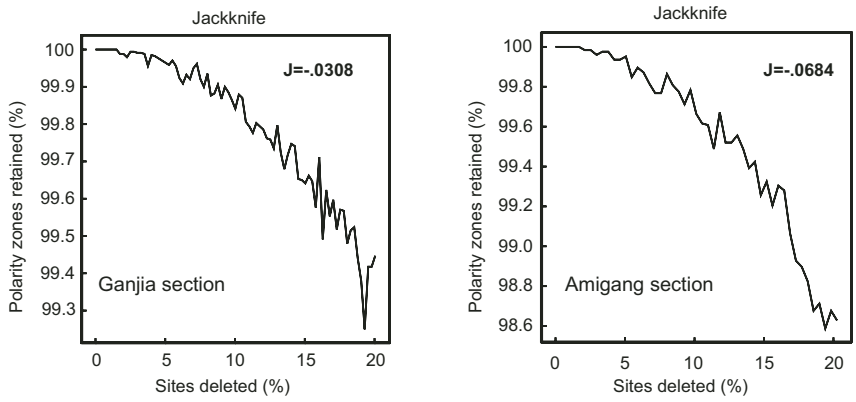

Figure 10. Magnetostratigraphic jackknife analysis (Tauxe and Gallet, 1991) for the Ganjia and Amigang sections. The plot indicates the relationship between average percent of polarity zones retained and the percentage of sampling sites deleted, where the slope J is directly related to the robustness of the results. The obtained slopes J have values of –0.0308 and –0.0684 in the Ganjia and the Amigang sections, respectively, which predict that the sections have recovered more than 95% of the true number of polarity intervals.

Miocene tectonic unrest. This unit was collected at the core of the "Guide Gate" structure; thus, we name unit 7 the Guidemen Formation.

Between units 7 and 8 a major angular unconformity is found. Unit 8 is characterized by tan, orange-red sandy gravel, sandstones and silty mudstones, which show strong lithological similarities to the strata of the Xining Group and the Tala Formation in adjacent basins (Li et al., 1997b; Editorial Commission for the Qinghai Provincial Stratigraphical Table, 1980). Because we did not include the strata of unit 8 in the present study, we have opted to leave the name as is (Xining Group). The Oligocene age we show in Table 1 for unit 8 is based on ostracoda and pollen (Qinghai Geology Bureau, 1989; Gu et al., 1992) and is supported by preliminary magnetostratigraphic work in progress (Yan et al., 2004).

DISCUSSION OF THE IMPLICATIONS FOR GUIDE BASIN EVOLUTION

The stratigraphic divisions introduced above reflect changes in the tectonosedimentary environment of the Cenozoic of the Guide basin (Fig. 11, Table 3). The (pre-Miocene) Xining Group (unit 8) represents a typical sedimentary cycle of upward fining sediments (sandy fine conglomerates to silty mudstones) forming in braided-river and overbank floodplain environments when the basin was initiated, in late Oligocene or earlier times (Song et al., 2001a). The onset of basin deposition was a result of flexing of the pre-Xining erosion surface and initial tectonic down-faulting along the margins of the surrounding mountains. This deeply weathered erosion surface is found on top of the Triassic and Precambrian basement, and truncates all pre-Cenozoic rocks. The thickness of the Xining Group appears to decrease southward from the southern margin of the Laji Shan toward the basin center, consistent with basin deposition taking place during continuous displacements along thrust faults at the basin's margins.

Before the thick package of conglomerates in the lower part of the Guidemen Formation began to be deposited (before the Burdigalian, i.e., before 20.4 Ma), we infer that a strong deformation phase occurred (Table 3), causing not only the clear angular unconformity between the Guide and Xining Groups, but also uplift of the surrounding mountains, such as the southward upthrusting of the Laji Shan along fault F2 (Fig. 3) or southwestward upthrusting along the nearby dextral Haiyan-Tongren transpressional fault (Fig. 1B). This deformation phase is recognized in the following two manners: (1) the Xining Group can be found beneath as well as on top of the Laji Shan basement complexes, and (2) the onset of fanglomeratic deposits of the lower Guidemen Formation during the early Burdigalian stage (ca. 20.8–19 Ma) marks a profound erosional phase that indicates uplift of the source areas of the conglomerate pebbles in the nearby Laji Shan. Rock types represented in the cobbles can be correlated with those in the Laji Shan.

Deposits of the Garang Formation in a braided-river environment followed the Guidemen Formation, and in turn were followed by the lacustrine Ashigong Formation (unit 5) in the middle-late Miocene (Song et al., 2001a). Then, during deposition of the Herjia Formation (unit 4; Messinian and early Pliocene), the sedimentary environment returned to that of a braided-river–overbank floodplain system (Fothergill, 1998; Song et al., 2001a), with slowly increasing sedimentation rates (up to ~20 cm/k.y.) (Fig. 11) and increasing pebble-conglomerate contents (Figs. 6 and 11). Whereas the early Miocene Guidemen conglomerates made a sudden appearance (Fig. 9), the Herjia Formation reveals a gradually increasing pebble conglomerate content during the interval ca. 7.8 Ma to 3.6 Ma (Fig. 11, dotted line), culminating in the boulder conglomerates of the Ganjia Formation at 3.6–2.6 Ma. The sedimentation rate (Fig. 11)

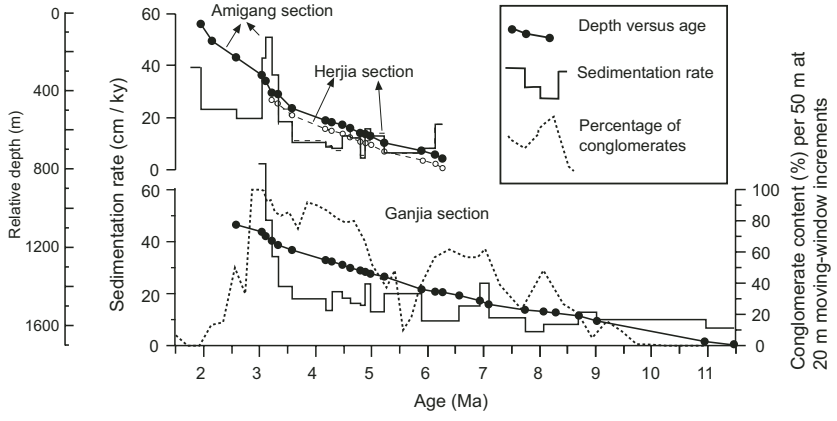

Figure 11. Depth versus age plots of the magnetic polarity chrons for three of the measured sections (with ages taken from the geomagnetic polarity time scale [GPTS] of Cande and Kent, 1995). Sedimentation rates (solid lines) are plotted as well, and so are percent occurrences of conglomerate beds (for the Ganjia Section only; dotted lines), calculated for each 50 m stratigraphic interval using 20 m moving-window increments.

increases dramatically at this mid-Pliocene time in both the Ganjia and Amigang sections, to more than 50 cm/k.y., with the deposition of conglomerates containing boulders up to 1 m in diameter in an alluvial–debris-flow fan system (Song et al., 2001a). The strata existing at that time were tilted some 8° to the south. The conglomerate deposition is not just a local phenomenon, as revealed by the occurrence of massive conglomerates of similar age elsewhere in northeastern Tibet (e.g., the Jishi Formation in the Longzhong Basin). This suggests an episode of vigorous deformation in the NE Tibetan Plateau, although contributions from climatic change cannot be ruled out (Zhang et al., 2001). We infer that this episode of late Pliocene tectonism accompanied the initiation of the south-verging thrusts F4 and F5, because the boulder conglomerates of the Ganjia Formation (3.6–2.8 Ma) are distributed only to the south of thrust F5 (Fig. 1B). We found soft red-bed detritus in the footwall, but could not unambiguously define this as having been derived from the Herjia or older formations in the hanging wall. The F4 and F5 thrusts and a splay F3 (Fig. 3) caused considerable shortening of the northeastern part of the Guide Basin between the Yellow River and the Laji Shan at this time.

From the Ganjia to the overlying Amigang Formation (unit 2), there is a sharp lithological change, in which massive boulder conglomerates give way to mostly siltstone and mudstone deposited in a lake system (Song et al., 2001a). A minor disconformity is present in the Ganjia section at the base of the Amigang Formation (Fig. 6), but not much time appears to be missing because the youngest normal interval of the Gauss Chron is represented almost completely in duration (as N1) in this section, as well as in the Amigang Section (N'3 in Fig. 6).

A distinctive feature of the Amigang Formation is that it contains the first appearance of Triassic slate pebbles. Because the Triassic source rocks are only distributed to the north of thrust F6 (Fig. 1B), whereas the Amigang Formation occurs only to the south of F6, it is suggested that thrusting along F6 was initiated or broke through to the surface at ca. 2.6 Ma, and caused the disconformity at this time (Fig. 6, Table 3). A northward tilt (~6°) of the Herjia Formation north of the Yellow River and a somewhat higher elevation of the north bank of the river suggest that thrust F6 near the town of Ashigong remained active until very recently.

The end of the lacustrine deposits of the Amigang Formation at ca. 1.8 Ma marks the transition of aggradation to degradation of the sedimentary basin fill. Fast incision of more than 900 m by the Yellow River after the Olduvai Subchron may indicate the (first?) appearance of the river in the Guide Basin and marks a Pleistocene episode of incision, deformation, and possibly uplift that continues until today, as can be deduced from the ages of the seven terraces of the Yellow River (T2–T7 in Figure 8 bottom; Li et al., 1997a).

TABLE 3. SUMMARY OF SEDIMENTARY ENVIRONMENTS OF THE GUIDE GROUP AND RELEVANT TECTONIC EVENTS

Time (Ma)	Sedimentary depositional environment	Typical sedimentation rate (cm/k.y.)		Tectonosedimentary events
Today	Eolian (loess)	~1		Degradation stage Yellow River incision of ~900 m
1.8	Shallow lacustrine—Amigang Formation	~20		Thrust F6
2.6	Massive boulder conglomerates throughout Northeastern Tibet—Ganjia Formation	~20–>50	↑ aggradation stage ↓	Minor unconformity Thrusts F4, F5; vigorous uplift and deformation
3.6	Coarser clastic, sand- to pebble-sized—Herjia Formation	~20		Increasing tectonism
7.0–7.8	Braided-river and lacustrine and overbank floodplain—Ashigong, Garang Formations	<10		Decreasing tectonism
Burdigalian	Pebble-sized conglomerates, alluvial fans—Guidemen Formation	~8		
Aquitanian	NA			Major angular unconformity Thrust F2
>20 Ma		NA		Folding and uplift

Note: Summary of sedimentary environments for the last 21 million years in the Guide Basin, the typical (averaged) sedimentation rates, and the relevant tectonic events that have been deduced from the Guide Group sediments and their magnetostratigraphically determined ages.

Combining our preliminary age estimates for the older part of the Guide Group (Fig. 9) with our recent field observations along the valley from Ashigong to Garang (Fig. 3), we can now begin to constrain the timing of the shortening in the northeastern Guide Basin, along the southern margin of the Laji Shan, i.e., along profile b–b′ of Figure 1B. It is estimated that the Guide Basin was initiated in the Oligocene, by analogy with the stratigraphy of the Linxia Basin and given the lithological similarities between the Xining Group and the late Oligocene Tala Formation (Fang et al., 2003). As already mentioned, and as summarized in Table 3, movement along F2 may have started in early Miocene time, movement along F4 and F5 occurred in the Pliocene after 3.6 Ma, and F6 is estimated to have become active in the early Pleistocene. This record of the timing of active thrusting in the basin indicates accelerated deformation during the Miocene, especially after the deposition of unit 5 (Ashigong Fm.), i.e., after ca. 8 Ma (see also Table 3).

Similar episodes of tectonic deformation and uplift in the NE Tibetan Plateau have been recorded in other nearby basins, such as the Linxia Basin ~150 km east of the Guide Basin (Fig. 1A), where detailed magnetostratigraphy demonstrates that flexuring of the basin occurred at ca. 29 Ma by southwest-northeast transpression along the dextral Leiji Shan fault west of Linxia (Fig. 1A) (Fang et al., 2003). This flexural subsidence continued to ca. 7 Ma when it began to decrease and when sedimentary strata started to be subject to folding. Red beds (mudstone and siltstone) in the Linxia Basin were truncated and folded ca. 4.0 Ma, followed by the thick boulder-conglomerate beds of the Jishi Formation (3.6–2.6 Ma) (Li et al., 1997b; Fang et al., 2003). Folding of the Jishi Formation occurred ca. 2.6 Ma and was followed by lake deposits of the Dongshan Formation until ca. 1.8 Ma, when degradation (i.e., erosion and incision) started in the Longzhong Basin (Li et al., 1997a, 1997b). The Dongshan-Jishi sequence of the Linxia Basin and the Amigang-Ganjia Formations of this study have similar ages, similar structural features such as unconformities, as well as similar lithologies, and they were deposited in similar environments. This not only indicates that both the Linxia and Guide Basins were subjected to nearly synchronous deformation and uplift under similar tectonic conditions, but also suggests that the beginning of the degradation phase of both basins is possibly related to the appearance of the Yellow River as it entered into the Longzhong and Guide basins at ca. 1.8 Ma by headward erosion.

On a larger scale, similar episodes of tectonism have been deduced for the late Oligocene, earliest and late Miocene, middle-late Pliocene, and early Pleistocene in the Qilian Shan–Altyn Tagh region (Gilder et al., 2001; George et al., 2001; Jolivet et al., 2001; Sobel et al., 2001; Song et al., 2001b; Yin et al., 2002; Wang et al., 2003), whereas in the Longmen Shan of the eastern Tibetan Plateau (at 32°N in Fig. 1A) a similar change in tectonic regime (from compressional to uplift and rapid exhumation) occurred in late Miocene–early Pliocene time as suggested by $^{40}Ar/^{39}Ar$ and (U-Th)/He thermal histories (Kirby et al., 2000).

CONCLUSIONS

Our magnetostratigraphic investigations of the Guide Basin provide detailed chronologic control for its late Miocene through early Pleistocene stratigraphy and allow us to propose a new lithostratigraphic division of the Guide Group. The Cenozoic sedimentary strata remain divided into two groups (Guide and Xining), but the Guide Group is now further divided into the Amigang, Ganjia, Herjia, Ashigong, Garang, and Guidemen Formations. Ages for the Amigang (1.8–2.6 Ma) and Ganjia (2.6–3.6 Ma) Formations are well established, whereas the lower age for the underlying Herjia is less precisely determined and can only be estimated as between 7.0 and 7.8 Ma. The ages for the Ashigong (older than 7.0 to older than 12 Ma), Garang (younger than 16 to 19? Ma) and the Guidemen (19?–20.8? Ma) Formations are at this time speculative best estimates. In this study we have not included the magnetic properties of the underlying Xining Group, thought to be Oligocene in age on the basis of sparse fossils, provisional magnetostratigraphy (Yan et al., 2004), and lithological correlations with well-dated strata in adjacent basins. A major episode of tectonic deformation and uplift has been demonstrated by significant shortening due to thrusting of faults F4 and F5, by a threefold increase in sedimentation rate, and by an increased influx of massive conglomerates at ca. 3.6–2.6 Ma. Similar boulder conglomerates, with nearly identical ages, have now been documented throughout northeastern Tibet and are interpreted to be the late Pliocene culmination of an accelerating tectonism that started ca. 8 Ma in the late Miocene.

Although it is difficult to date movements along thrusts with great confidence, we estimate that the thrusting started as early as Oligocene (F1) and continued with movements on thrust F2 in the early Miocene, followed by thrusting farther south at 3.6 Ma (F4 and F5) and again after 2.6 Ma (F6).

ACKNOWLEDGMENTS

This work has been funded to the Chinese researchers by the National Science Foundation of China (NSFC) (#40334038, 40121303) and the Chinese Academy of Science (RJZ[2002]005), and by the U.S. National Science Foundation, Division of Earth Sciences, grant EAR-9903074 to R. Van der Voo and J.M. Parés, as well as through grants from the University of Michigan's Scott Turner Fund to M. Yan (2001, 2002). We would like to thank Dong Sun, Xianhai Xu, Denglin Gao, Shengli Yang, Hongbo Jin, Weilin Zhang, Yunfa Miao, and the late William Downs for extensive help with field and laboratory work. Thanks are also due to Professor Qiu Zhanxiang for his help in identifying the fossil mammals found in the Guide Basin, and Professor Rixiang Zhu for his help with the use of the 2G cryogenic magnetometer. The journal's reviewers, Clark Burchfiel and Guillaume Dupont-Nivet, and Associate Editor Ken Kodama, are thanked for making many valuable suggestions for improvement.

REFERENCES CITED

Berggren, W.A., and Van Couvering, J.A., 1974, The late Neogene: Biostratigraphy, geochronology, and paleoclimatology of the last 15 million years in marine and continental sequences: Palaeogeography, Palaeoclimatology, Palaeoecology, v. 16, p. 1–216.

Bohlin, B., 1937, Ober-Oligozäne Säugetiere aus dem Shargaltein–Tal (Western Kansu): Sino- Swedish Expedition, Palaeontology Sinica, New Series C: Whole Series, v. 107, p. 1–66.

Burchfiel, B.C., Deng, Q., Molnar, P., Royden, L., Wang, Y., Zhang, P., and Zhang, W., 1989, Intracrustal detachment zones of continental deformation: Geology, v. 17, p. 748–752.

Burchfiel, B.C., Zhang, P., Wang, Y., Zhang, W., Song, F., Deng, Q., Molnar, P., and Royden, L., 1991, Geology of the Haiyuan fault zone, Ningxia-Hui Autonomous region, China, and its relation to the evolution of the northeastern margin of the Tibetan Plateau: Tectonics, v. 10, p. 1091–1110.

Cande, S.C., and Kent, D.V., 1995, Revised calibration of the geomagnetic polarity time scale for the Late Cretaceous and Cenozoic: Journal of Geophysical Research, v. 100, p. 6093–6095.

Chen, Z., Burchfiel, B.C., Liu, Y., King, R.W., Royden, L.H., Tang, W., Wang, E., Zhao, J., and Zhang, X., 2000, Global Positioning System measurements from eastern Tibet and their implications for India/Eurasia intercontinental deformation: Journal of Geophysical Research, v. 105, p. 16,215–16,227.

Delville, N., Arnaud, N., and Montel, J.M., 2001, Paleozoic to Cenozoic deformation along Altyn-Tagh fault in the Altun Shan massif area, eastern Qilian Shan, northeast Tibet, China, *in* Hendrix, M.S., and Davis, G.A., eds., Paleozoic and Mesozoic tectonic evolution of central Asia: From continental assembly to intracontinental deformation: Geological Society of America Memoir 194, p. 269–292.

Dupont-Nivet, G., Horton, B.K., Butler, R.F., Wang, J., Zhou, J., and Waanders, G.L., 2004, Paleogene clockwise tectonic rotation of the Xining-Lanzhou region, northeastern Tibetan Plateau: Magnetostratigraphic and biostratigraphic results: Journal of Geophysical Research, v. 109 (B4).

Editorial Commission for the Qinghai Provincial Stratigraphical Table, 1980, Qinghai Provincial Handbook: Beijing, Geology Press (in Chinese), p. 190–194.

Fang, X.M., Garzione, C., Van der Voo, R., Li, J.J., and Fan, M.J., 2003, Flexural subsidence by 29 Ma on the NE edge of Tibet from the magnetostratigraphy of Linxia Basin, China: Earth and Planetary Science Letters, v. 210, p. 545–560.

Fang, X.M., Zhao, Z.J., Li, J.J., Yan, M.D., Pan, B.T., Song, C.H., and Dai, S., 2004, Paleomagnetism of the late Cenozoic stratigraphy in the Jiuxi Basin north of the Qilian Mountains and uplift of the Tibetan Plateau: Science China D, v. 34, no. 2, p. 97–106.

Fothergill, P.A., 1998, Late Tertiary and Quaternary intermontane basin evolution in north-east Tibet: The Guide Basin [Ph.D. thesis]: London, London University, 228 p.

Fothergill, P.A., and Ma, H., 1999, Preliminary observations on the geomorphic evolution of the Guide Basin, Qinghai Province, China: Implications for the uplift of the northeast margin of the Tibetan Plateau, *in* Smith, B.J., Whalley, W.B., and Warke, P.A., eds., Uplift, erosion and stability: Perspectives on long-term landscape development: Geology Society of London Special Publication 162, p. 183–200.

Garcés, M., Agustí, J., Cabrera, L.l., and Parés, J.M., 1996, Magnetostratigraphy of the Vallesian (late Miocene) in the Vallès-Penedès (NE Spain): Earth and Planetary Science Letters, v. 142, p. 381–396.

Gaudemer, Y., Tapponnier, P., Meyer, B., Peltzer, G., Guo, S., Chen, Z., Dai, H., and Cifuentes, I., 1995, Partitioning of crustal slip between linked, active faults in the eastern Qilian Shan, and evidence for a major seismic gap, the 'Tianzhu gap', on the western Haiyuan fault, Gansu (China): Geophysical Journal International, v. 120, p. 599–645.

George, A.D., Marshallsea, S.J., Wyrwoll, K., Chen, J., and Lu, Y., 2001, Miocene cooling in the northern Qilian Shan, northeastern margin of the Tibetan Plateau, revealed by apatite fission-track and vitrinite-reflectance analysis: Geology, v. 29, p. 939–942.

Gilder, S., Chen, Y., and Sen, S., 2001, Oligo-Miocene magnetostratigraphy and rock magnetism of the Xishuigou section, Subei (Gansu Province, western China) and implications for shallow inclinations in central Asia: Journal of Geophysical Research, v. 106, p. 30,505–30,521.

Gu, Z., Bai, S., Zhang, X., Ma, Y., Wang, S., and Li, B., 1992, Neogene subdivision and correlation of sediments within the Guide and Hualong basins of Qinghai province: Journal of Stratigraphy, v. 16, p. 96–104.

Horton, B.K., Dupont-Nivet, G., Butler, R.F., Wang, J., Zhou, J., and Waanders, G.L., 2004, Mesozoic-Cenozoic evolution of the Xining-Minhe and Dangchang basins, northeastern Tibetan Plateau: Magnetostratigraphic and biostratigraphic results: Journal of Geophysical Research, v. 109 (B4).

Jolivet, M., Brunel, M., Seward, D., Xu, Z., Yang, J., Roger, F., Tapponnier, P., Malavieille, J., Arnaud, N., and Wu, C., 2001, Mesozoic and Cenozoic tectonics of the northern edge of the Tibetan Plateau: Fission track constraints: Tectonophysics, v. 343, p. 111–134.

Kirby, E., Whipple, K.X, Burchfiel, B.C., Tang, W., Berger, G., Sun, Z., and Chen, Z., 2000, Neotectonics of the Min Shan, China: Implications for mechanisms driving Quaternary deformation along the eastern margin of the Tibetan Plateau: Geological Society of America Bulletin, v. 112, p. 375–393.

Li, H.B., Yang, J.S., Xu, Z.Q., Wu, C.L., Wan, Y.S., Shi, R.D., Liou, J.F., Tapponnier, P., and Ireland, T.R., 2002, Geological and chronological evidence of Indo-Chinese strike-slip movement in the Altyn Tagh fault zone: Chinese Science Bulletin, v. 47, no. 1, p. 27–32.

Li, J.J., Fang, X.M., Van der Voo, R., Zhu, J.J., MacNiocaill, C., Ono, Y., Pan, B.T., Zhong, W., Wang, J.L., Sasaki, T., Zhang, Y.T., Cao, J.X., Kang, J.C., and Wang, J.M., 1997a, Magnetostratigraphic dating of river terraces: Rapid and intermittent incision by the Yellow River of the northeastern margin of the Tibetan Plateau during the Quaternary: Journal of Geophysical Research, v. 102, p. 10,121–10,132.

Li, J.J., Fang, X.M., Van der Voo, R., Zhu, J.J., MacNiocaill, C., Cao, J.X., Zhong, W., Chen, H.L., Wang, J.L., Wang, J.M., and Zhang, Y.T., 1997b, Late Cenozoic magnetostratigraphy (11–0 Ma) of the Dongshanding and Wangjiashan sections in Longzhong Basin, western China: Geologie en Mijnbouw, v. 76, p. 121–134.

Li, Y.L., and Yang, J.C., 1998, Tectonic geomorphology in the Hexi Corridor, north-west China: Basin Research, v. 10, p. 345–352.

Métivier, F., Gaudemer, Y., Tapponnier, P., and Meyer, B., 1998, Northeastern growth of the Tibetan Plateau deduced from balanced reconstruction of two depositional areas: The Qaidam and Hexi Corridor basins, China: Tectonics, v. 17, no. 6, p. 823–842.

Meyer, B., Tapponnier, P., Bourjot, L., Métivier, F., Gaudemer, Y., Peltzer, G., Guo, S., and Chen, Z., 1998, Crustal thickening in Gansu-Qinghai, lithospheric mantle subduction, and oblique, strike-slip controlled growth of the Tibet Plateau: Geophysical Journal International, v. 135, p. 1–47.

Molnar, P., and Lyon-Caen, H., 1989, Fault plane solutions of earthquakes and active tectonics of the Tibetan Plateau and its margins: Geophysical Journal International, v. 99, p. 123–153.

Pan, B., 1994, Research upon geomorphologic evolution of the Guide Basin and the development of the Yellow River: Arid Land Geography, v. 7, no. 3, p. 43–50.

Parés, J.M., Van der Voo, R., Downs, W.R., Yan, M., and Fang, X.M., 2003, Northeastward growth and uplift of the Tibetan Plateau: Magnetostratigraphic insights from the Guide Basin: Journal of Geophysical Research, v. 108, p. 1–11.

Qinghai Geology Bureau, 1989, Regional geology of Qinghai Province: Beijing, Geology Press, p. 215–217 (in Chinese).

Qiu, Z.X., and Qiu, Z.D., 1995, Chronological sequence and subdivision of Chinese Neogene mammalian faunas: Palaeogeography, Palaeoclimatology, Palaeoecology, v. 116, p. 41–70.

Ritts, B., and Biffi, U., 2000, Magnitude of post–Middle Jurassic (Bajocian) displacement on the central Altyn Tagh fault system: Geological Society of America Bulletin, v. 112, p. 61–74.

Roberts, A.P., and Lewis-Harris, J.C., 2000, Marine magnetic anomalies: Evidence that 'tiny wiggles' represent short-period geomagnetic polarity intervals: Earth and Planetary Science Letters, v. 183, p. 375–388.

Sobel, E., Arnaud, N., Jolivet, M., Ritts, B.D., and Brunel, M., 2001, Jurassic to Cenozoic exhumation history of the Altyn Tagh range, northwest China, constrained by $^{40}Ar/^{39}Ar$ and apatite fission track thermochronology, *in* Hendrix, M.S., and Davis, G.A., eds., Paleozoic and Mesozoic tectonic evolution of central Asia: From continental assembly to intracontinental deformation: Geological Society of America Memoir 194, p. 247–267.

Song, C.H., Fang, X.M., Gao, J.P., Sun, D., and Fan, M.J., 2001a, Cenozoic tectonic uplift and sedimentary evolution of the Guide Basin in the northeast margin of the Tibetan Plateau: Sedimentology, v. 19, no. 4, p. 498–506.

Song, C.H., Fang, X.M., Li, J.J., Gao, J.P., and Fan, M.J., 2001b, Tectonic uplift and sedimentary evolution of the Jiuxi Basin in the northern margin of the Tibetan Plateau since 13 Ma BP: Science China, v. 44, Supplement, p. 192–202.

Song, C.H., Fang, X.M., Gao, J.P., Nie, J.S., Yan, M.D., Xu, X.H., and Sun, D., 2003, Magnetostratigraphy of late Cenozoic fossil mammals in the northeastern margin of the Tibetan Plateau: Chinese Science Bulletin, v. 48, p. 188–193.

Tapponnier, P., Meyer, B., Avouac, J.P., Peltzer, G., Gaudemer, Y., Guo, S., Xiang, H., Yin, K., Chen, Z., Cai, S., and Dai, H., 1990, Active thrusting and folding in the Qilian Shan and decoupling between upper crust and mantle in northeastern Tibet: Earth and Planetary Science Letters, v. 97, p. 382–403.

Tapponnier, P., Xu, Z., Roger, F., Meyer, B., Arnaud, N., Wittlinger, G., and Yang, J., 2001, Oblique stepwise rise and growth of the Tibet Plateau: Science, v. 294, p. 1671–1677.

Tauxe, L., 1998, Paleomagnetic principles and practice: Dordrecht, Kluwer Academic Publishers, 299 p.

Tauxe, L., and Gallet, Y., 1991, A jackknife for magnetostratigraphy: Geophysical Research Letters, v. 18, p. 1783–1786.

Wang, X., Wang, B., and Qiu, Z., 2003, Danghe area (western Gansu, China) biostratigraphy and implications for depositional history and tectonics of northern Tibetan Plateau: Earth and Planetary Science Letters, v. 208, p. 253–269.

Yan, M.D., Van der Voo, R., Fang, X.M., Parés, J.M., Rea, D.K., and Song, C.H., 2004, Neogene magnetostratigraphy of the Guide Basin: Mid-Miocene clockwise rotation and implications for uplift of the NE Tibetan Plateau: Geological Society of America Abstracts with Programs, Abstract 18-13, v. 36, no. 5, p. 50.

Yin, A., Rumelhart, P.E., Butler, R., Cowgill, E., Harrison, T.M., Foster, D.A., Ingersoll, R.V., Zang, Q., Zhou, X.Q., Wang, X.F., Hanson, A., and Raza, A., 2002, Tectonic history of the Altyn Tagh fault system in northern Tibet inferred from Cenozoic sedimentation: Geological Society of America Bulletin, v. 114, p. 1257–1295.

Zhai, Y., and Cai, T., 1984, The Tertiary system of Gansu Province, *in* Gansu geology: Lanzhou, People's Press of Gansu, p. 1–40 (in Chinese).

Zhang, P., Burchfiel, B.C., Molnar, P., Zhang, W., Jiao, D., Deng, Q., Wang, Y., Royden, L., and Song, F., 1991, Amount and style of late Cenozoic deformation in the Liupan Shan area, Ningxia Autonomous region, China: Tectonics, v. 10, p. 1111–1129.

Zhang, P., Molnar, P., and Downs, W.R., 2001, Increased sedimentation rates and grain sizes 2–4 Myr ago due to the influence of climate change on erosion rates: Nature, v. 410, p. 891–897.

Zheng, S., Wu, W., Li, Y., and Wang, G., 1985, Late Cenozoic mammalian faunas from the Guide and Gonghe basins, Qinghai Province: Vertebrata PalAsiatica, v. 23, p. 89–134.

Manuscript Received by the Society 22 September 2004
Revised Manuscript Received 15 February 2005
Manuscript Accepted 16 February 2005

Printed in the USA